University of Alberta

Characterization of Clay Minerals and Kerogen in Alberta Oil Sands Geological End Members

by

Limin Zheng

A thesis submitted to the Faculty of Graduate Studies and Research
in partial fulfillment of the requirements for the degree of

Master of Science

in

Chemical Engineering

Department of Chemical & Materials Engineering

Fall 2013

Edmonton, Alberta

Abstract

The high degree of variability of oil sands ores can be attributed to a mixture of different geological end members, i.e., estuarine sand, estuarine clay, marine sand and marine clay. This study focused on the mineralogy, especially of clay minerals, and toluene insoluble organic matter, referred to as kerogen, in different oil sands end members. Clays and kerogens will likely have a significant impact on solvent recovery from the gangue following non-aqueous bitumen extraction.

The bitumen-free solids were subjected to mineralogical and geochemical analysis. Kerogens were isolated and analyzed by various characterization methods. The types of clays were identified in oriented samples by X-ray diffraction analysis. The nitrogen to carbon ratio in the isolated kerogens is found to be higher than in bitumen. There are more type III kerogens in estuarine samples and more type II kerogens in marine samples.

Acknowledgements

First of all, I would like to sincerely thank my supervisors Dr. Qi Liu, Dr. Thomas Etsell and Dr. Douglas Ivey for their guidance and support during my research. Being a student supervised by them was a most gratifying experience. They encouraged my interest with full trust. Their enlightened and critical suggestions are greatly appreciated.

Secondly, I would take the chance to thank my colleges Mirjavad Geramian and Marek Osacky. They helped me a lot in starting this research, especially during clay characterization. I really enjoyed the pleasant work experience.

Thirdly, I want to thank the Centre for Oil Sands Innovation (COSI) for financial support and Syncrude Energy Ltd. for the samples. Also, thanks to Keith Draganiuk and Xiaoli Tan for the operational training for various instruments in the COSI labs. Thanks to Shihong Xu for his help during XPS analysis, Martin Kupsta for the FIB sample preparation and Dr. Hamed Sanei from the Geological Survey of Canada for the Rock-Eval analysis and fluorescence microscopy.

Last, but not least, I would like to thank my parents and all my friends for being there with me and giving me confidence to overcome difficulties in life and study.

Table of Contents

List of Tables

List of Figures

1 Introduction

The proven recoverable oil reserves in Canada are 170 billion barrels, 97% of which are in the oil sands. Alberta's oil sands are found in three deposits - Athabasca, Peace River and Cold Lake (CAPP, 2012). Athabasca oil sands were formed in the McMurray Formation. During the long dynamic geological history, the McMurray Formation was formed in terrestrial, estuarine and marine environments successively, corresponding to the lower, middle and upper intervals of the McMurray Formation, respectively (Ranger and Gingras, 2007; Ranger and Pemberton, 1997). The oil sands are mixtures of different geological end members. The terrestrial deposit provides a minor amount of ore. The major geological members mined at the Syncrude's North Mine and Aurora Mine sites are estuarine and marine ores. In each geological interval, clays and oil sands are interbedded in each other. The marine ore interval is usually shallow, so the estuarine ore is the main production interval. In estuarine ore, the clays are pale and grey in color. However, although marine sands and marine clays are interbedded like estuarine ore, marine clays are as black and dark as marine sands.

The properties of oil sands in various mining sites and the recovery of bitumen using non-aqueous extraction may be attributed to a combination of the properties of the different geological end members, i.e., estuarine sand (ES), estuarine clay (EC), marine sand (MS) and marine clay (MC). Although the current commercial oil sands operations are based on warm water extraction of bitumen (Masliyah et al., 2011), non-aqueous extraction of the oil sands bitumen has been studied for

quite a long time (Benson, 1969; Gantz and Hellwege, 1977). Recently, Hooshiar studied the non-aqueous extraction procedure and characterized the clay minerals in the solvent extraction products (Hooshiar et al., 2012); Nikakhtari found that the most viable solvent for non-aqueous bitumen extraction is cyclohexane (Nikakhtari et al., 2012). The mineralogy of oil sands geological end members was characterized (Osacky et al., 2013) with regards to non-aqueous extraction. The differences were rooted in the diverse mineralogy and organic petrology, with clays and kerogens being the primary indicators. Expandable and non-expandable clays in oil sands are unlikely to act similarly during non-aqueous bitumen extraction due to their different properties (Geramian et al., 2012).

Kerogen is insoluble in common organic solvents. The definition of kerogen varies in different disciplines. In the Alberta oil sands industry, kerogen can be considered to be the toluene insoluble organic matter that is left associated with the mineral solid residues after the Dean-Stark extraction procedure. Clays and kerogens in the Alberta oil sands may significantly affect bitumen extraction from the oil sands by a non-aqueous solvent, as well as the recovery of the solvent from the extraction gangue. In this study, the mineralogy was determined and the types of clays were identified in the oil sands geological members. Kerogens from these end members were isolated and characterized to develop a fundamental understanding of insoluble organics in the oil sands, with the objective of assisting the development of a viable non-aqueous oil sands bitumen extraction process.

2 Literature Review

2.1 Geology and formation of Alberta oil sands

Alberta's oil sands are found in three deposits - Athabasca, Peace River and Cold Lake. The oil sands exist at the surface in the Athabasca area but deeper underground in other areas. Geologically, Athabasca oil sands mainly exist in the McMurray Formation (Su et al., 2013). The McMurray Formation is a stratigraphical unit of Cretaceous age in the Western Canadian Sedimentary Basin. During the long history of the dynamic environment, the McMurray Formation was formed in terrestrial, estuarine and marine environments successively, corresponding to the lower, middle and upper intervals of the McMurray Formation (Ranger and Gingras, 2007; Ranger and Pemberton, 1997). The mineralogy and organic matter formed in disparate geological periods vary greatly.

Oil sands display a high heterogeneity in various deposits and areas. The heterogeneity is the result of different portions of geological sediments that formed in different environments. In the Alberta oil sands, the heterogeneity can be attributed to a combination of different oil sands end members, i.e., terrestrial sand, terrestrial clay, estuarine sand, estuarine clay, marine sand and marine clay. However, in the surface mining sites of Syncrude's deposits, mainly in the Athabasca region, terrestrial ore is present in a minor amount and only exists locally. The estuarine sediments are the main oil sands regions with oil impregnation. Within the ore, black, bitumen-rich estuarine sands and grey, laminated estuarine clays are interbedded. They can be easily distinguished and

separated. However, although marine ores are also composed of interbedded sands and clays, the marine clays are as black as the marine sands and are difficult to separate.

The geology of Alberta's oil sands and the formation and migration of bitumen have been studied for a long time. Garven (1989) proposed that tectonic uplift of the western part of the Alberta basin caused a topography-driven flow system to develop shortly after maximum burial. Topographic relief drove basinal fluids through petroleum source rocks into the underlying Upper Devonian carbonates from the Rocky Mountains to the erosional edge of the basin. Adams et al. (2004) reproduced Garven's model and suggested that a comprehensive simulation would have to consider the transience of driving forces (compaction, buoyancy, capillary forces and hydrodynamic flow), including the development of surface topography and three-dimensional spatial distribution of permeability through time (Adam et al., 2004).

2.2 Oil sands extraction technologies

1) Surface mining and hot water extraction

In typical surface mining, oil sands are mined and crushed; hot water and additives are added to prepare slurries up to 55ºC. The slurry is fed into hydro-transport pipelines. Primary separation vessels (PSV) are used to recover bitumen from the middling streams. The aerated bitumen rises to the top of the separation vessel to form bitumen froth. The bitumen froth is de-aerated and then fed to the bitumen froth treatment plant to remove solids and water. The Clark hot water

extraction process is still in use by Syncrude and Suncor as the primary bitumen extraction technology. Hot water extraction became profitable due to technology development, such as hydrotransportation, the world's largest hauling trucks, hydraulic shovels and cyclofeeders. The final technology platform, called Natural Froth Lubricity, allowed for the pumping of bitumen froth without the need for froth cleanup (Masliyah et al., 2011).

2) In-situ bitumen extraction

In terms of the massive bitumen amount, 315 billion barrels in place, with 170 billion barrels recoverable with current technology, about 20% is accessible through surface mining, while 80% requires in-situ methods, such as the cyclic steam stimulation (CSS) process developed by Imperial Oil Ltd. at Cold Lake and the steam assisted gravity drainage (SAGD) process developed by the Alberta Oil Sands Technology and Research Authority (AOSTRA) and industry partners. However, there are still oil sands reserves too deep for surface mining but not deep enough for in-situ mining. In-situ technology unlocks the potential to recover large reserves that cannot be accessed economically by traditional mining methods. No additional surface or groundwater is required and no tailings ponds are created. The SAGD process is the leading in-situ extraction method. In this process, parallel pairs of horizontal wells are drilled: one for steam injection and one for oil recovery. The injector well is about five meters above the producer well (Masliyah et al., 2011).

3) Non-aqueous bitumen extraction

Although the surface mining and in-situ processes have been successfully applied commercially, the extensive mining and extraction of bitumen from oil sands has caused many environmental problems, including a large amount of water consumption, land disturbance, tailings ponds footprint and green-house gas emissions. Among these issues, tailings treatment has caused increasing concern in recent years. Oil sands tailings are a mixture of water, sands, fine clays, silts, residual bitumen and other by-products of oil sands mining and extraction processes. However, because of the stable suspension of fines and oil in the tailings ponds and the formation of mature fine tailings (MFT), settling and reclamation of the tailings ponds region may take several decades. Currently, the total area of existing tailing ponds is more than 170 km^2 and is growing rapidly (Pembina Institute report, 2013), which is an urgent problem that needs to be solved.

Along with the two technological processes currently used in oil sands extraction in the Alberta area, another technology has been proposed, namely non-aqueous bitumen extraction. It is still in the laboratory stage and progress has been made. Dantz and Hellwege (1977) patented the use of trichloroethylene as a solvent; Leung and Phillips found that solvents with high aromaticity or low boiling points show higher mass transfer rates. Naphtha was also studied in a water aided solvent extraction process (Sparks and Meadus, 1988; Hooshiar, et al., 2012) studied a non-aqueous bitumen extraction procedure and found that, unlike the water extraction process, the solvent extraction procedure was not sensitive to the fines and clay contents of the oil sands ores or to the ore grade, at least for

medium and high-grade ores. Nikakhtari et al. (2012) developed a non-aqueous bitumen extraction process and screened different light hydrocarbon solvents, including aromatics, cycloalkanes, biologically derived solvent and mixtures of solvents. They found cyclohexane to be a viable solvent for non-aqueous bitumen extraction after this screening operation. Cyclohexane has higher bitumen extraction efficiency and evaporates faster compared to other solvents, which makes it feasible for non-aqueous bitumen extraction.

The solvent extraction process requires much lower fresh water consumption and energy input, thus avoiding the generation of large tailings ponds and green-house gas emissions. It is a promising technology that needs further study.

2.3 Oil sands mineralogy

Oil sands are mixtures of sands, clay, water, extremely viscous bitumen and insoluble organics, referring to as kerogen. In the oil sands industry, it is generally recognized that the coarse sands do not cause any problem throughout the extraction process. However, the fines (<44μm) content plays an important role during the oil extraction process. Bitumen recovery decreases with increasing fines content (Chong, et al., 2003) in warm water extraction. Wik, et al. (2008) illustrated that small particle size is a contributing factor affecting bitumen recovery but comparison tests with ultra-fine silica particles (<0.3 μm) showed that mineralogy is a more important parameter. Nano- and micro-size minerals, mainly clay minerals, are most detrimental (Hooshiar et al., 2012; Eslahpazir, et al. 2011). These minerals may interact with the solvent, bitumen and connate water

due to their small particle size, high specific surface area, swelling capacity, cation exchange capacity, layer charge and specific physicochemical properties.

2.3.1 Types of clays and clays in oil sands

The definitions of clay are not unified in all disciplines. Most recently, clay has been defined as a naturally occurring material composed primarily of fine-grained minerals, which is generally plastic at appropriate water content and will harden on drying and firing (Guggenheim and Martin, 1995).

Although particle size is a key parameter in the definition of clay, there is no generally accepted maximum size (Bergaya, 2006). There are many types of clays in nature. Based on their structure, the clay minerals can be classified into two groups, 1:1 layer group (e.g., kaolin group) and 2:1 layer group (e.g., illite/mica, smectite, vermiculite and chlorite). Generally, clays are fundamentally built of silica tetrahedral sheets and alumina octahedral sheets, as described in the structure section below.

Clays can be categorized depending on the way that tetrahedral and octahedral sheets are packed into layers. If there is only one tetrahedral and one octahedral sheet in each layer, the clay is known as 1:1 clay, Figure 1-1. The unit cell of the 1:1 layer structure includes six octahedral sites and four tetrahedral sites. The alternative, known as the 2:1 clay, shown in Figure 1-2， has two tetrahedral sheets with the unshared vertex of each sheet pointing towards each other and forming the octahedral sheet between them. Six octahedral sites and eight tetrahedral sites characterize the 2:1 layer unit cell (Bergaya et al., 2006).

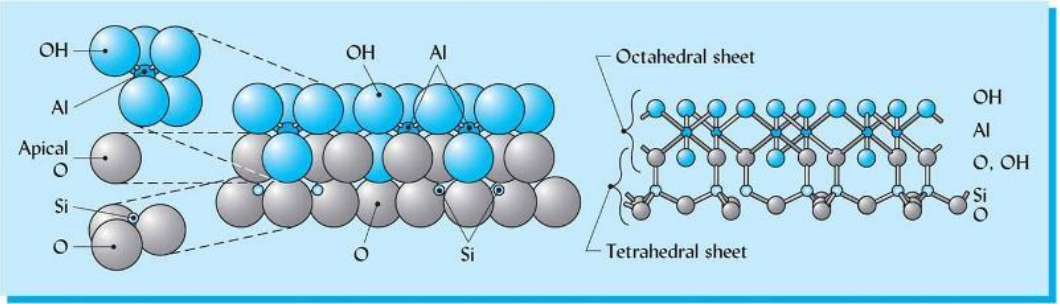

Figure 2-1 Structure of group 1:1 clays (AGS 105 soils).

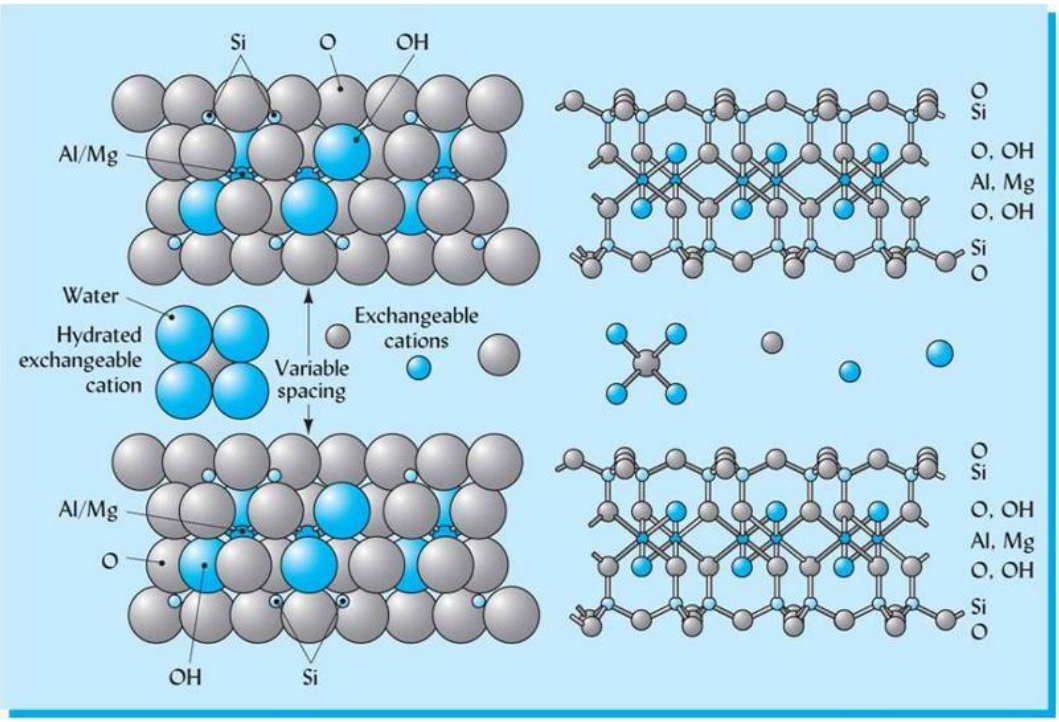

Figure 2-2 Structure of group 2:1 clays (AGS 105 soils).

There are four general groups of minerals with 2:1 type crystal structures (AGS 105 soils). In the fine-grained mica group, about 20% of the silicon atoms in the tetrahedral sheets have been replaced by aluminum and the very strong negative charge resulting is satisfied by potassium ions held rigidly between adjoining 2:1 layers and preventing expansion of the crystal.

Two clay groups with 2:1 type structures have expansive type crystals, the smectites and vermiculites. The individual 2:1 layers are held together only loosely and exchangeable cations and water molecules are attracted between the layers resulting in enormous internal adsorptive surfaces. Consequently, these clays expand when wet and shrink when dry and have very high cation adsorption capacities. In the smectite group, magnesium has substituted for some of the aluminum in the octahedral sheet and - aluminum has substituted for some of the silicon in the tetrahedral sheet. The vermiculite group is less expandable than the smectite group, since water and magnesium ions act as bridges holding the 2:1 type layers together. Vermiculites have very high cation adsorption capacities due to significant substitution of aluminum for silicon in the tetrahedral sheets as well as some substitution of magnesium for aluminum in the octahedral sheet.

Another 2:1 type mineral, chlorite, is non-expansive since its interlayer between two 2:1 layers is occupied by a magnesium-dominated octahedral sheet that holds the adjacent layers together. Chlorite has particle size, cation adsorption capacity, and physical properties similar to those of fine-grained micas. Figure 1-3 shows the structures of 1:1 clay-kaolinite and four 2:1 clay groups and demonstrates the reasons for expandability.

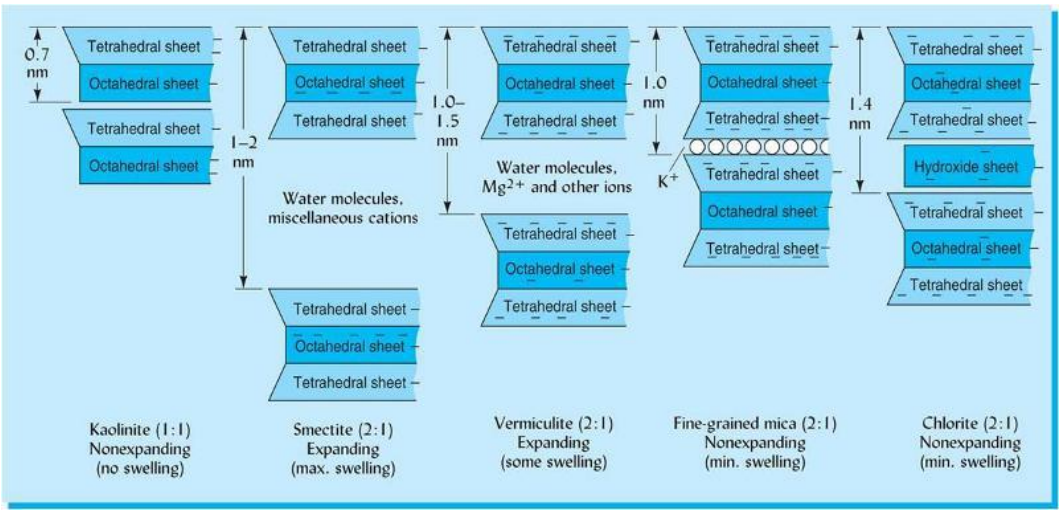

Figure 2-3 Schematic drawing illustrating the organization of tetrahedral and octahedral sheets in one 1:1-type mineral (kaolinite) and four 2:1-type minerals (AGS 105 soils).

The mineralogy of clay minerals in the Alberta oil sands has been studied and a summary of these studies can be found in papers by Kaminsky et al. (2009) and Omotoso and Mikula (2004). Based on such studies, the mineralogy of clay minerals in the Alberta oil sands deposit varies across the deposit. Kaolinite, illite, smectite and chlorite are found to be the major clay minerals in the Alberta oil sands deposits with the first two being the most abundant.

2.3.2 Identification and quantification of clay minerals in oil sands

Clay minerals are difficult to identify and quantify because of their great structure diversity. Clay identification of powdered oriented samples by X-ray diffraction (XRD) remains - the standard technique. Quantitative analysis is performed to obtain the quantity of clay minerals in bulk samples. XRD is the most commonly used method, but infrared spectroscopy (IR) and major element analysis combined with quantitative XRD are also applied (Bergaya, 2006). Because clay varies

greatly in chemical composition and structure, analytical errors are usually very large. Consequently, in most cases, the results are semi-quantitative. The overall success of quantitative analysis depends on sample preparation, data processing and standards selection (Środoń, 2002). Quantitative XRD with the RockJock program has been used by Osacky et al. (2013) to analyze the mineralogical composition of Alberta oil sands.

Quantitative XRD with the RockJock program (Eberl, 2003) provides a good method to quantify clay minerals in oil sands. RockJock is a computer program that determines quantitative mineralogy, for example, quartz and feldspar, as well as clay, in powdered bulk samples by comparing the integrated X-ray diffraction peak intensities of individual minerals in complex mixtures to the intensities of an internal standard, corundum.

The RockJock program has been applied by Osacky et al. to analyze different geological end members from Alberta oil sands (Osacky et al., 2013).The calculations of the RockJock program are based on three previously published methods: (1) the matrix flushing technique of Chung (1974), in which integrated intensities of the unknown minerals are compared to that of an internal standard (in the case of RockJock, corundum), thereby obviating the need for measuring the mass absorption coefficient for a sample;(2) the whole-pattern fitting routine of Smith and others (Smith et al., 1987) for measuring integrated intensities by fitting the sum of pure mineral patterns to that of the measured XRD pattern; and (3) the quantitative method of Srodon and others (Srodon et al., 2001) for sample preparation, and for the method of measuring clay mineral content from non-basal

reflections rather than from the more commonly used basal reflections (Eberl, 2003).

2.4 Occurrence of organic matter in oil sands

The origins of petroleum can be classified into two categories: organic and inorganic origins. The inorganic theory is that acetylene (C_2H_2) is formed through a reaction of carbides with water, and the acetylene, in turn, forms petroleum.

The organic origin of petroleum is currently widely accepted even though it is still somewhat controversial. In the organic formation theory, living organisms die and decompose; then most are recycled by other organisms and decomposed to small molecules, while the rest are preserved in forms of organic matter in sediments during burial.

Kerogen formed at mild temperatures and pressures in young sediments is metastable. Without further burial, kerogen may remain stable. As sedimentation and burial proceed, kerogen is subjected to progressively higher temperature and pressure environments. It is no longer stable under the new conditions and rearrangement occurs during the successive stages of diagenesis, catagenesis, and metagenesis toward thermodynamic equilibrium (Adams et al., 2004). During successive burial of kerogen, it will be arranged and will evolve correspondingly, during which time oil, gas and bitumen can be released.

In terms of petroleum exploration, the diagenesis stage corresponds to immature kerogen and little hydrocarbon is generated in the source rocks. The stage of

catagenesis corresponds to the main zone of oil generation and also to the beginning of the cracking zone with a rapidly increasing proportion of methane. However, the stage of metagenesis is entirely situated in the dry gas zone.

Origins of kerogen in Alberta oil sands are different in successive historical environments, i.e., terrestrial, estuarine and marine sediments. Macerals are the individual organic components making up kerogen and they are classified by optical properties determined by organic petrology. Examples of macerals are liptinite, vitrinite and inertinite. They are determined by the type of organic material from which the macerals are derived. Liptinite macerals are considered to be produced from decayed leaf matter, spores, pollen and algal matter. Resins and plant waxes can also be part of liptinite macerals. Vitrinite is considered to be composed of cellular plant material such as roots, bark, plant stems and tree trunks. Inertinite is highly oxidized and equivalent to charcoal. Terrestrial sedimentary organics contain a large amount of vitrinite, while marine sediments rarely have vitrinite. However, if formed in severe environments, some terrestrial sediments may not be suitable for plants, so it may rarely contain vitrinite. On the other hand, lipitinite can be present in all kinds of sediments.

2.4.1 Types of kerogen

Kerogen, the insoluble organic matter, is formed during the burial process of organic matter. With increasing temperature and pressure, kerogen is rearranged and generates and releases hydrocarbons, such as oil, gas and bitumen. During burial, kerogen evolves continuously and the amounts of hydrogen and oxygen

decrease. Because kerogen is generated from various sources, the degradation paths are different. The most useful classifications of kerogen types are based on hydrogen, carbon and oxygen ratios of the organic matter (Peters and Moldowan, 1993).

Type I kerogen has a high atomic hydrogen to carbon (H/C) ratio and a low atomic oxygen to carbon (O/C) ratio. It is predominantly composed of the most hydrogen-rich organic matter known in the geological record. The organic matter is often amorphous alginite of algal or bacterial origin. In other circumstances, some Type I kerogens are morphologically distinct and can be assigned to a specific type. Type I kerogens consist mostly of liptinite macerals with minor amounts of vitrinite and inertinite sometimes present.

Type II kerogen has high atomic H/C and low O/C ratios compared with Types III and IV. It originates from mixtures of zooplankton, phytoplankton and bacterial debris in marine sediments. Type II kerogens are dominated by liptinite macerals with lesser amounts of vitrinite and inertinite.

Type III kerogen has low H/C and high O/C ratios. Such low hydrogen organic matter is polyaromatic and derived mostly from higher plants. Type III kerogen is the chemical equivalent of vitrinite and huminite and, thus, is called humic or woody kerogen. It produces natural gas and occasionally the associated condensate if the thermal maturation is adequate.

Type IV kerogen has a low H/C ratio and a relatively high O/C ratio. Usually it is oxidized and hydrogen-poor. It cannot be a source of petroleum.

Table 2-1 lists the origins and the oil/gas potentials for each type of kerogen.

Table 2-1 Maceral groups and oil/gas potential in different kerogen types (Peters and Cassa, 1994)

Kerogen Type	**Maceral Group**	**Oil/Gas Potential**
I	Morphous alginite	oil
II	liptinite	oil
II/ III	liptinite/vitrinite	mixed oil and gas
III	vitrinite	gas
IV	inertinite	none

To determine the types and maturity of kerogen, van Krevelen plots of atomic H/C ratio versus O/C ratios have been used (van Krevelen, 1961).

However, construction of the van Krevelen diagram is time consuming and expensive. Thus it is not favourable for onsite drilling operations or screening large sample populations. A quicker and less expensive method is employed in a Modified van Krevelen diagram using Rock-Eval parameters and total organic carbon (TOC) analysis. The Modified van Krevelen diagram plots atomic hydrogen index (HI) versus oxygen index (OI). The three kerogen types mature along different evolutionary paths with the arrows pointing towards higher maturity states (Figure 2-4).

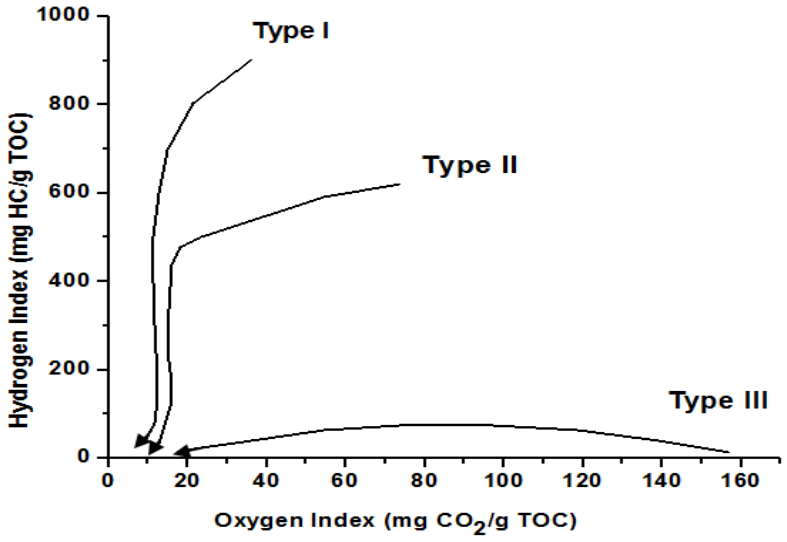

Figure 2-4 Modified van Krevelen diagram (Peters and Moldowan, 1993).

2.4.2 Kerogen characterization methods

1) Total organic carbon and total nitrogen determination

Carbon content in sediments is the direct indicator of organic matter content. There is organic carbon and inorganic carbon. To determine the organic carbon content in sediments, some pretreatment should be done to destroy the inorganic carbon. Usually acid is used to eliminate the carbonate in the sediments. The acid should not be too strong to oxidize other minerals or too weak to react with carbonate.

In soil analysis, H_2SO_3 is frequently used to eliminate the carbonate. After acid treatment, the samples are subjected to dry combustion to determine the organic carbon content (Skjemstad and Baldock, 2006). If the total carbon is also determined, the total inorganic carbon can be obtained by difference.

Another standard method for total organic carbon analysis is to use phosphoric acid combined with a carbon analyzer to determine total organic carbon, total inorganic carbon and total carbon (Bernard et al., 2009).

2) Rock-Eval pyrolysis

Rock-Eval pyrolysis is a popular and easy operating method used for the analysis of rocks in oil and gas exploration. This technique uses a programmed temperature increase to heat a sample (rock ~70 mg, coal ~50 mg). It generates three peaks during the heating and cooling process. It is a two-step process.The samples are first pyrolyzed in an inert atmosphere and two peaks are generated: S1 and S2 (mg hydrocarbon/g dry rock). S1 is generated from the free oil already in the rock. S2 is generated from the release of hydrocarbon during thermal cracking of kerogen in the rock.A flame ionization detector (FID) is used to record the S1 and S2 peaks. During the pyrolysis step, peak S3 can be measured continuously by infrared (IR) spectroscopy. Carbon monoxide (CO) and carbon dioxide (CO_2) contribute to the S3 signal. $S3CO_2$ (mg CO_2/g) and S3CO (mg CO/g) are measured and are derived from oxygen-containing organics. The sample is then transferred to an oxidizing chamber and heated to 850°C, burning off all remaining organic matter (OM); the fourth peak S4 can now be recorded (Carrie et al., 2012; Sanei et al., 2005). The pyrolysable carbon (PC) is computed from S1, S2 and S3, and residual carbon (RC) from S4. The total organic carbon (TOC) is calculated by taking the sum of the PC and the RC.

Hydrogen index (HI) (mg hydrocarbon from S2 per g TOC) versus oxygen index (OI) (mg of CO_2 from S3 per g TOC) can be calculated based on Rock-Eval results. HI ((S2/TOC)×100) is the ratio of S2 hydrogen (in mg hydrocarbon per g dry rock) to total organic carbon (TOC). OI ((S3/TOC)×100) is the ratio of S3 oxygen (mg CO_2 per g dry rock) to TOC. Consequently, T_{max} is a standardized parameter. It is the temperature at which the S2 peak reaches its maximum. It is used as a parameter to determine the maturity of source rocks. T_{max} = 400ºC - 435ºC represents immature organic matter; T_{max} = 435ºC - 470ºC represents a mature or oil zone; T_{max} > 470ºC represents the postmature zone (Hunt, 1996), where there is no potential to form oil and gas.

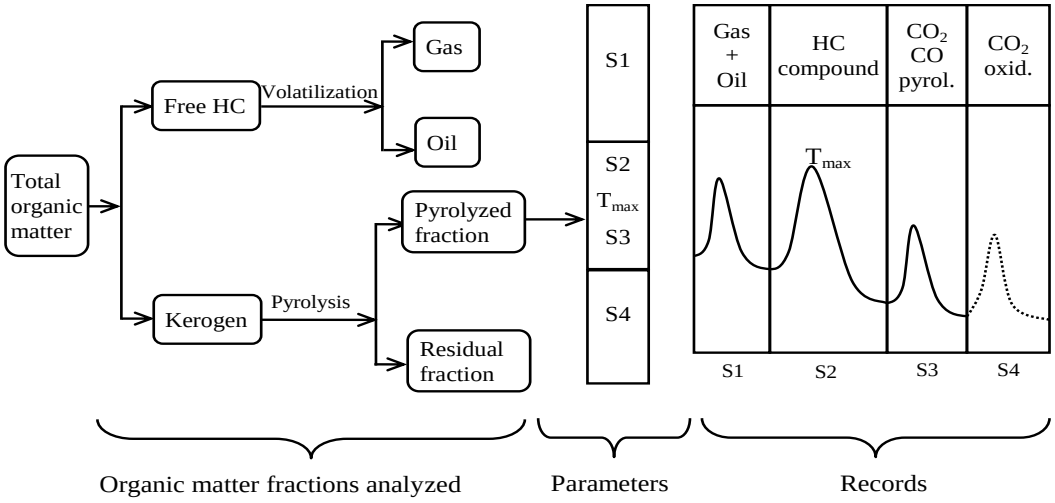

Figure 2-5 General diagram showing the different fractions of total organic matter of rocks, the corresponding parameters and recordings in Rock-Eval analysis (Lafargue et al., 1998)

Figure 2-5 is a general diagram showing the fractions of organic matter in sediments and corresponding parameters and recordings.

Parameters obtained by Rock-Eval analysis are used to plot in the Modified van Krevelen diagram, shown in Figure 2-4. The Modified van Krevelen diagram is used to determine the type and maturity of kerogen. The arrows point toward higher maturation states and represent continuous burial. The Modified van Krevelen method is a faster and less expensive method than the van Krevelen method, which is time consuming and expensive.

3) Kerogen isolation

There are many methods that can be used to separate kerogen from its mineral matrix (Durand, 1980). These methods can be categorized into physical methods and chemical methods. Among physical methods, flotation, ultrasonic, electromagnetic and electrostatic methods can be used. These methods are applied after fine grinding of the sediment. The chemical properties of the kerogen are preserved without alteration of the kerogen structure. The recovery of kerogen varies widely based on different sources. Physical methods are not very effective to isolate most of the kerogen from the matrix.

In chemical methods, the objectives are to dissolve the mineral matrix and preserve the original structure of kerogen as much as possible. Acid treatment is performed after grinding the samples. To eliminate minerals from the sediments, HCl and HF are used to dissolve carbonates, sulfides, sulfates, oxides, hydroxides and silicates. A temperature sufficient to dissolve all carbonates but not high enough to cause oxidation is needed, typically 60-70ºC. The minerals are sometimes protected from chemical attack by organic matter. Acid attack cannot

dissolve all minerals such as pyrite, which is the most commonly occurring residual mineral in the obtained kerogen. Most of the other minerals are present in small quantities and are stable. During HF attack, there is frequently neoformation of complex fluorides. The fluorides may interfere with the organic matter during further analysis, e.g., elemental analysis.

After physical or chemical separation, there is usually still a certain amount of inorganic residue associated with the kerogen; this inorganic residue will affect further analysis of the kerogen, e.g., elemental analysis and ^{13}NMR analysis. These residual heavy minerals can be separated by density separation which is currently widely used. Macerals of ancient sedimentary organic matter, comprising lipinite, vitrinites and inertinite, have been separated by sequential centrifuging in zinc bromide solutions of progressively increasing specific gravities. Kinghorn and Rahman, (1980) separated different maceral groups of organic matter dispersed in sedimentary rocks by this technique. Marine organic matter, composed of structureless platy constituents, is separated by low-density, heavy-liquid solutions (SG = 1.2-1.34), whereas material from terrestrial and land influenced sources separates out at higher specific gravities (SG = 1.45- 1.65). The density increases of the obtained kerogen were accompanied by a darkening of their colour, from yellow to brown and then to black, reflecting increasing maturity (Kinghorn and Rahman, 1980).

4) Elemental analysis

Elemental analysis determines the amount of an element in a compound. There are many different experimental methods for determining elemental composition, generally for carbon, hydrogen and nitrogen. This type of analysis is especially useful for organic compounds. During elemental analysis, a sample is burned in an excess of oxygen, and various traps collect the combustion products - carbon dioxide, water, and nitric oxide. The masses of these combustion products can be used to calculate the composition of the sample. During the analysis of bitumen and heavy oil, because of their high sulfur content, sulfur analysis is also required. The Vario Micro Cube elemental analyzer consists of an O_2 closing unit, a furnace reaction cube and a detector. The pressure in the instrument ranges from 120 to 125 kPa. A balance is used to automatically transfer the sample weight to the operating software. Each sample is put in an alumina boat; the boat is then closed in oxygen atmosphere, and put on the sample carousel. Samples are transferred into the furnace in sequence where upon the outside air is displaced. The combustion tube and reduction tube with constant temperatures, 1150°C and 850°C, respectively, are held in a furnace. In the combustion tube, the sample is burned with oxygen, at a flow rate of 14 mL/min, to form N_2, NO_x, CO_2, H_2O, SO_2 and SO_3 gases. In the reduction tube, NO_x and SO_3 are reduced to N_2 and SO_2. The separator consists of an adsorption column. A thermal conductivity detector (TCD), which consists of a measuring and reference cell, is used for detection. Helium is used as the carrier gas, with a flow rate of 200 mL/min; the flow rate is measured with a mass flow controller (MFC)-TCD flow meter. The signal is

digitized and integrated. The weight content of each element can be calculated using the supplied software.

In some cases, oxygen content is needed for the compounds. The Modified Unterzaucher method is the most widely used for oxygen content determination (Oliver, 1995). The sample is weighed in a silver capsule and dropped inside the reactor furnace maintained at around 1000°C where the sample is pyrolyzed. Quantitative conversion of oxygen to carbon monoxide (CO) is achieved by a layer of nickel coated carbon. The pyrolyzed gas mixture flows through a chemical trap to remove other acidic gases and water. The gas then enters a chromatographic column heated for separation of the CO from nitrogen (N_2). The CO is measured using a thermal conductivity detector, which produces an electrical signal proportional to the concentration. Calibration of the instrument is achieved by using commercially available organic analytical standards.

X-ray fluorescence spectroscopy (XRF) is another elemental analysis method in use. XRF is a non-destructive and fast method to analyze various samples, e.g., solids, liquids, powders and slurries. The fluorescence of X-rays can be used to detect the abundance of certain atoms, heavier than sodium, in the sample. X-rays are a high energy and high frequency form of electromagnetic radiation. Under X-ray irradiation, atoms become excited and unstable. An outer shell electron can replace an inner shell electronand the energy difference between the two orbits is released. The energy difference between electron orbits is known and fixed, so every type of atom has its own characteristic radiation spectrum.

5) Scanning electron microscopy (SEM) analysis

Since the 1960s, the development and application of scanning electron microscopy has continued (Khursheed, 2011). When energetic electrons strike the sample, a variety of signals are generated, and it is the detection of specific signals which produces an image or a sample's elemental composition. SEM can provide high resolution topographical and morphological surface images if combined with a secondary electron (SE) detector. It can also provide atomic number contrast images if combined with a backscattered electron (BSE) detector. Elemental maps and spot chemical compositions can be acquired with the assistance of an energy dispersive X-ray (EDX) spectrometer.

Secondary electrons are emitted from the atoms occupying the top surface and produce an interpretable image of the surface. The contrast in the image is determined by the sample morphology.

Backscattered electrons are primary beam electrons which are scattered by the atoms in the solid. The contrast in the image produced is determined by the atomic number of the elements in the sample. The image will, therefore, show the distribution of different chemical phases in the sample. Because these electrons are emitted from deeper within the sample, the resolution in the image is not as good as for secondary electrons.

EDX can provide rapid qualitative, or with adequate standards, quantitative analysis of elemental composition with a sampling depth of 1-2 microns. Interaction of the primary beam with atoms in the sample causes shell transitions

which result in the emission of an X-ray. The emitted X-ray has an energy characteristic of the parent element. Detection and measurement of the energy permits elemental analysis. X-rays may also be used to form maps or line profiles, showing the elemental distribution in a sample surface.

A typical SEM column, operating in a vacuum, consists of an electron gun, a condenser lens system, an objective lens, a set of deflectors and an electron detection system, i.e., SE, BSE and EDX detectors. The electron gun provides a source of electrons and accelerates them to energies ranging from <1 keV to 30 keV. The electron beam interacts with the surface of the sample to a depth of approximately 1 μm. Secondary electrons have low energies, less than 50eV, while backscattered electrons have energies from 50eV to the primary beam energy.

6) Transmission electron microscopy (TEM) and focused ion beam (FIB) sample preparation

Transmission electron microscopy (TEM) is a microscopic technique, with the capability of imaging at a significantly higher resolution than light microscopy. Objects on the order of a few angstroms (10^{-10} m) can be examined. An electron source emits electrons that travel through an evacuated column of the microscope. The electrons are focused into a fine beam by electromagnetic lenses. The electron beam then travels through an electron transparent specimen. Because electrons are low-mass, negatively charged particles, they can be easily deflected by the electrons or the positive nucleus of an atom. Depending on the density of

the material present, some of the electrons are scattered from the main beam. Below the specimen the unscattered (or scattered) electrons hit an imaging device, such as fluorescent screen. The image can be studied directly by the operator or photographed with a camera. An EDX detector is complimentary attachment to the TEM. The data generated by EDX analysis consist of spectra showing peaks corresponding to the elements making up the true composition of the sample being analysed.

Using the TEM technique, Oberlin et al. (1980) investigated the microtexture of kerogen, and Largeau et al. (1990) observed ultra-laminar structures in amorphous kerogens.

With the help of advanced sample preparation (Sisk et al., 2010), the study of nanopore structures and pore fillings in solids became visible. Focused ion beam (FIB) systems use a finely focused beam of ions (usually gallium) that can be operated at low beam currents for imaging or high beam currents for site specific sputtering or milling. Focused ion beam (FIB) techniques can be used to prepare a flat surface of the samples for both SEM and TEM analysis. FIB techniques can serve as a sample preparation method assisting TEM analysis. A thin section of the region of interest is prepared using FIB, which is then characterized using TEM imaging, electron diffraction, and X-ray microanalysis. The method is particularly useful for identifying low concentrations of metals and their compounds (Eslahpazir et al., 2011) in solids.

7) X-ray photoelectron spectroscopy (XPS)

X-ray photoelectron spectroscopy (XPS) is a quantitative spectroscopic technique and surface chemical analysis technique that measures elemental composition of the surface (top 1-10 nm), surface contamination, chemical or electronic states of each element on the surface, elemental composition line profiling and depth profiling. XPS spectra are obtained by irradiating a material with a beam of monochromatic X-rays while simultaneously measuring the kinetic energy and number of electrons that escape from the top 1 to 10 nm of the material being analyzed. XPS requires ultra-high vacuum conditions.

XPS provides a good method, when combined with other methods, i.e., elemental analysis, Fourier transform infrared spectroscopy (FTIR) and nuclear magnetic resonance (NMR), to understand the chemical structure of complex organics, such as kerogen, coal and bitumen. XPS offers a way to investigate directly organic bonds and the forms of inorganic oxygen, sulfur and nitrogen in complex carbonaceous materials such as kerogen (Kelemen et al., 2007).

8) Fluorescence microscopy

Optical or light microscopy, including transmission and reflective microscopy, has long been used to image sedimentary organic matter (Durand, 1980). Recent studies on organic petrology are widely conducted using incident light microscopy equipped with white and fluorescent light sources (Sanei et al., 2005; Zaccone et al., 2011) to visually see the organic evolution path and maceral structures. The light can be switched from white light to fluorescent light. Optical microscopy can be used together with Rock-Eval analysis to better understand

different types of organics (e.g., bitumen, coal and kerogen) in sediment rocks based on light reflectance, fluorescence, structure and color by comparison under white and fluorescence light. The fluorescent light microscope has long been used in the characterization of organic matter in sediments. Fluorescence light microscopic observation was used to differentiate among several types of amorphous particles (Chang and Huang, 2008; Senftle, 1986). However, this method should be used with caution, because mature amorphous organic matter does not exhibit fluorescence (Durand, 1980). Therefore, the organic matter is usually examined by both fluorescent and transmitted light microscopes (Sawada et al., 2012). Dozens of images in depth can be obtained and stacked into one image to overcome drawbacks from surface roughness.

2.5 Objectives of this research

This research mainly focuses on the mineralogy and kerogen in Athabasca oil sands geological end members, with the objective to assist the development of a non-aqueous extraction process. Non-aqueous bitumen extraction has been studied for a long time and progress has been made, but it has not been well developed and commercially applied.

As illustrated in Section 2.1, the heterogeneity of Alberta oil sands can be attributed to a combination of different oil sands end members, i.e., estuarine sand, estuarine clay, marine sand and marine clay. Mineralogy and kerogen in different geological end members varies significantly.

Clays and kerogens existing in the matrix of the oil sands are believed to affect bitumen recovery and solvent recovery, and they first need to be qualitatively and quantitatively characterized to see the differences in different geological end members. Clay minerals widely exist in the oil sands (Hooshiar et al., 2012). They have fine sizes, high specific surface areas, layer/edge charges, exchangeable cations and flexible layers. Based on these properties, they are generally considered as a colloidal material capable of aggregation and gelation in solvents and water. When associated with bitumen, clays can be both water and oil wetted and thus will suspend in solvents. The suspension can cause serious problems in the bitumen extraction process. It is already well known that in water-based oil sands extraction, the bitumen froth contains a significant amount of fines. Also, the mature fine tailings (MFT) are a serious issue for the reclamation of tailings ponds.

Organic matter in oil sands end members can be divided into two groups: toluene soluble and toluene insoluble organic matter, namely bitumen and kerogen, respectively. Dean-Stark soxhlet extraction using hot toluene is the standard method to determine bitumen content in oil sands (Bulmer and Starr, 1979). However, there is still a certain amount of organic matter remaining in the solids after Dean-Stark extraction. To avoid interference with the determination of bitumen, the toluene insoluble organic matter is specified as kerogen.

This research qualitatively and quantitatively characterized the clays and kerogens in oil sands geological end members. Interactions of clay-bitumen and kerogen-bitumen need to be further studied to understand their behavior during non-

aqueous bitumen extraction in order to assist the development of the non-aqueous extraction process.

3 Experimental Materials and Methodologies

3.1Materials and preparation

3.1.1 Samples and sample preparation

The four oil sands geological end members, estuarine sand (ES), estuarine clay (EC), marine sand (MS) and marine clay (MC), were obtained from Syncrude's Aurora Mine and North Mine sites. The end members were carefully separated manually, split into sub-samples and stored in a freezer. Before using, the samples were removed from the freezer and thawed to room temperature overnight. Then the samples were ground using a mortar and pestle to pass a 60 mesh sieve, which gives a particle size around 250 μm. Extraction was done using toluene separately for 24 hours to remove all the bitumen from the samples. A standard Dean-Stark procedure (Bulmer and Starr, 1979) was followed; about 120 g of sample was used and the procedure was repeated twice for each sample. The oil sands end member samples after the Dean-Stark procedure were collected and designated as ESAD, ECAD, MSAD and MCAD.

Kerogens were isolated from the bitumen-free solids by HF/HCl treatment, and these samples were designated as K-ESAD, K-ECAD, K-MSAD, K-MCAD. Details of the isolation method are described later in section 3.2.4. The kerogen samples were further density separated by a zinc bromide ($ZnBr_2$) solution with specific gravity (SG) of 1.65, as described in Section 3.2.5. The density separated kerogen samples were marked as K-ECAD-f, K-ECAD-f, K-MSAD-f and K-MCAD-f, where the suffix "f" denotes the "float" fraction. The bitumen extracted

from the four geological end members was marked as Bitumen-ESAD, Bitumen-ECAD, Bitumen-MSAD and Bitumen-MCAD.

3.1.2 Chemicals

1. Toluene (Certified ACS). Toluene was used in the Dean-Stark bitumen extraction process.

2. Fume HF, 70% (w/w) HF in H_2O. HF was used during the kerogen isolation, as described in Section 3.2.4.

3. Concentrated 37% (w/w) and 5% (v/v) HCl aqueous solution. HCl was used in the kerogen isolation, described in Section 3.2.4, and also the density separation process, as described in Section 3.2.5.

4. Zinc bromide ($ZnBr_2$), anhydrous, 98%. $ZnBr_2$ solution (SG = 1.65) was used in the density separation process; Section 3.2.5 describes how to prepare the $ZnBr_2$ solution.

3.2 Methodologies

3.2.1 X-ray diffraction (XRD) and quantitative X-ray diffraction (Q-XRD)

Oil sands end members were prepared for quantitative XRD and the RockJock program analysis to determine their mineralogical compositions. Random samples were prepared according to Omotoso's method (Omotoso and Eberl, 2009), which was modified from Środoń's technique (Środoń et al., 2001). Oriented samples were prepared by dispersing approximately 150mg of powder (<2μm fraction) in

2mL distilled water and then pipetting the suspension onto a glass slide and drying at room temperature. The dried glass slides were equilibrated overnight at 54% relative humidity (RH) over a saturated solution of $Mg(NO_3)_2$ prior to XRD analysis. The saturated solution of $Mg(NO_3)_2$ kept the relative humidity at 54%. Oriented prepared samples, which were air dried (54% RH) and then vapor saturated with ethylene glycol at 60°C for 12 hours, were analyzed by XRD. The ethylene glycol was used to expand the expandable clay minerals. XRD patterns of these oriented preparations were used for identification of the clay minerals (Osacky et al., 2013).

A Rigaku rotating anode XRD system, with CuKα radiation and a graphite monochromator, was used for the analysis of oil sands end members. It was operated at 40 kV. The step size for all analyses was 0.02°2θ/sec from 4 to 65°2θ (Osacky et al., 2013).

Quantitative X-ray diffraction (QXRD) was performed on random preparations using RockJock (Version 11) software (Eberl, 2003). RockJock determines the quantitative content of the minerals in powdered samples by comparing the integrated reflection intensities of the individual minerals with the intensities for pure standard minerals and an internal standard (corundum). Each sample was passed through a 250 μm sieve. Then 1.000 g of sample was mixed with 0.250 g of corundum and ground with 4 mL of ethanol in a McCrone micronizing mill for 5 min using zirconia grinding cylinders. The mixture was dried overnight at about 80°C. The sample/corundum mixture was then shaken in a plastic vial (25 mL) with 3 plastic balls (9 mm diameter) using a Retsch MM 200 mill. DuPont™

Vertrel® 191 XF, as a grinding aid, was added to the mixture in the ratio of 0.5 mL Vertrel to 1 g of solids and the vial was shaken for 10 min. The powder was passed through the 250 μm sieve again and side loaded into an XRD holder against frosted glass by gently tapping the holder on a hard surface. Frosted glass was used during the preparation to make sure the sample settled randomly. Samples were scanned in the X-ray diffractometer from 4 to 65°2θ. The X-ray diffraction intensities extracted from the XRD files using Jade software were entered into the RockJock program and the mineral composition (wt%) was calculated.

3.2.2 Total organic carbon content determination

To compare the reliability of organic carbon measurements, a CHNS Vario Micro Cube elemental analyzer and a Costech 4010 Elemental Analyzer System were used to determine organic carbon content.

For the Vario Micro Cube method, first about 100 mg of sample, W_o, was loaded into a combustion boat, H_3PO_4 solution (85%) was added drop by drop until all the sample was wetted by the solution, the sample was placed in the oven at 50ºC overnight, the sample was washed by distilled water five times using millipore filtration, and then returned to the oven at 50ºC until dry. The sample was collected and homogenized. The weight of the sample after acid treatment was recorded, W_f. The Vario Micro Cube was then used for the elemental analysis; about 20 mg was used each time and five tests were done for each sample; details

are given in Section 3.2.6. The average of the carbon content was obtained, C_a. The total carbon content was calculated, $C = C_a \times (W_f / W_o)$.

For the Costech 4010 method, an oil sands sample, about 100 mg and with known moisture content, was passed through a 100 mesh sieve and collected into a nonporous combustion boat that had been previously ignited and cooled. Based on the estimate of inorganic carbon present, the sample was treated with an excess of 6% H_2SO_3 solution. After several hours, the water and excess H_2SO_3 were removed by leaving the boat overnight in an evacuated desiccator containing NaOH pellets. The sample was dried overnight and analyzed by the dry combustion method using a Costech 4010 Elemental Analyzer System.The carbon content of the acid treated sample was reported as the organic carbon content (Nelson and Sommers, 1996).

3.2.3 Rock-Eval analysis

Rock-Eval 6® was used for geochemical analysis. The procedure for the Rock-Eval analysis consisted of two processes:

1. The sample was first heated in an inert atmosphere (helium). The sample was heated at 300°C for 10 minutes and then to 650°C at a heating rate of 25°C/min. During the pyrolysis process, the quantity of free, 'volatile' hydrocarbons present in the sample (S1 peak, mg hydrocarbons per g of sample) and the amount of hydrocarbons released by the thermal cracking of OM (S2; mg hydrocarbons per g of sample) were detected by a flame ionization detector (FID). Simultaneously, the CO and CO_2 released during thermal cracking of oxygen-bearing organic

compounds (S3; mg CO–CO_2 per g of sample) were measured by online infrared (IR) detectors. The measurement of CO was conducted up to 570°C, while the measurement of CO_2 was conducted up to 400°C. This is to avoid interference from the release of inorganic CO and CO_2 at temperatures higher than 570 and 400°C, respectively (Sanei et al., 2005).

2. The sample was automatically transferred to the oxidation oven where it was heated from 400 to 850°C in air, incinerating all the residual organic carbon in the sample. During this step, the CO and CO_2 released during combustion of residual organic carbon (S4; mg CO–CO_2 per g of sample) were measured by online infrared (IR) detectors. The quantity of all organic matter released during pyrolysis (pyrolysable carbon, 100-650 °C) and oxidation (residual carbon, 400-850 °C) accounts for the total organic carbon (TOC, wt%) in the sediment sample.

3.2.4 Kerogen isolation

The oil sands end members, i.e., ES, EC, MS and MC, were prepared for kerogen isolation. A chemical isolation method was chosen to isolate as much kerogen as possible while trying to keep the kerogen structure intact. The oil sands end member samples were first ground to pass a 60 mesh sieve. They were then subjected to soxhlet extraction for 24 hours to remove all the bitumen in the samples. 120g of the original solid was used each time for Dean-Stark extraction.

Six samples were utilized, i.e., ESAD, ECAD, EC, MSAD, MCAD and MC. Each sample, around 100 mg in size, was placed in the isolation apparatus and treated with concentrated HCl for 3 hours. The samples were then rinsed four times to

remove any dissolved Ca ions. The residues from HCl treatment were subsequently treated with 70% HF and agitated for at least two days. Fresh HF was added to the slurry on the second day, accompanied with heating for 3 h at 50°C to ensure that the samples were in strong (fuming) HF. The leached residues were rinsed to neutral pH (pH=7). Afterwards, a small amount of HCl was added and the pulp was heated for 3 hours at 50°C to dissolve any fluorosilicates. The resulting solid residues (kerogen) were rinsed to neutral pH and freeze dried.

3.2.5 Density separation

Zinc bromide (100 g) was diluted by the addition of 5% hydrochloric acid to obtain a solution with a specific gravity of 1.6. Kerogen was added to the density solution and centrifuged for about 30 minutes at 7000 rpm. The "float" fraction (kerogen) was decanted and washed two times with 5% HCl and three times with distilled water. The sample was then freeze dried. This method was applied to all the kerogen samples.

3.2.6 Elemental analysis

AVario Micro Cube elemental analyzer was used to determine the CHNS content of the solids, bitumen and kerogen samples. Oxygen was determined with a Carlo Erba EA1108 elemental analyzer, which is based on a modified Unterzaucher method. The samples analyzed using this method include the geological end members before bitumen removal; EC and MC end members after bitumen extraction; ESAD, ECAD, MSAD and MCAD; kerogen isolated from these four geological end members: K-ESAD, K-ECAD, K-MSAD and K-MCAD; kerogen

after density separation: K-ESAD-f, K-ECAD-f, K-MSAD-f and K-MCAD-f; bitumen extracted by Dean-Stark from the four geological end members: Bitumen-ESAD, Bitumen-ECAD, Bitumen-MSAD and Bitumen-MCAD.

First, the Vario Micro Cube elemental analyzer and operating software were started. Then all the parameters in the software were initiated and the software was prepared for analysis. Next about 20 mg of solid sample and 2 mg of bitumen were loaded into an aluminium boat. Finally the boat was sealed in an O_2 environment and put into the sample pan. Each sample was repeated 4~5 times. Once started, the content of each element (C, H, N and S) was calculated automatically; details were given in Section 2.7. The average value is reported.

For oxygen content analysis using the Carlo Erba EA1108 Elemental Analyzer, the sample was weighed (0.5 mg) in a silver capsule and dropped inside the reactor furnace maintained at 1040ºC (1070ºC is optimal, but the furnace available could not go that high) where the sample was pyrolyzed. Quantitative conversion of oxygen to carbon monoxide (CO) was achieved by a layer of nickel coated carbon. The pyrolyzed gas mixture flowed through a chemical trap to remove acidic gases and H_2O. The gas then entered a chromatographic column (molecular sieve 5A) heated at 70ºC for separation of the CO from N_2. The CO was measured using a thermal conductivity detector, which produced an electrical signal proportional to the concentration. Calibration of the instrument was achieved by using commercially available organic analytical standards. Four samples of stearic acid (0.2, 0.6, 1.0 and 1.6 mg) were used as standards to create a calibration curve. Approximately 0.5 mg of each sample were analyzed each

time; the analysis was repeated three times for each sample and the average calculated.

3.2.7 X-ray fluorescence spectroscopy (XRF)

An EDAX Orbis XRF spectroscope, with a Rh X-ray source, was used. Isolated kerogen samples were subjected to XRF to detect the heavy elements in the samples. Around 150 mg of kerogen powders were pressed (20,000 kPa for 2 min) into pellets. Regions 2 mm in size for each sample were used for this analysis. The XRF was operated at a high voltage of 40 kV and a current of 750 μA within the Rh tube. The live time was 30 seconds. Only elements heavier than sodium are detectable in XRF. The total mass content of the elements was normalized to 100 percent based on the detectable elements, so the weight percent obtained by XRF was not the actual percentage in the sample. Sulfur content was analyzed by CHNS elemental analysis and served as a standard to calculate the actual mass composition of each sample. For example, the sulfur content may have been 5 wt% by CHNS analysis and 10 wt% by XRF analysis. Because 5 wt% was considered as the actual sulfur content in the sample, all the element contents obtained by XRF were corrected by dividing by 10%/5% = 2.

3.2.8 Scanning electron microscopy (SEM)

To determine the morphology and to identify the heavy elements associated with the isolated kerogen, a Hitachi S2700 scanning electron microscope (SEM) equipped with a PGT PRISM IG (intrinsic Ge) detector for EDX analysis was used. A Zeiss EVO® MA 15 LaB6 filament SEM, operated at 20 kV, was also

used for higher resolution BSE and SE images. Kerogen powders were dispersed on carbon tape and then coated with gold prior to SEM analysis to prevent charging.

3.2.9 Transmission electron microscopy (TEM) and focused ion beam (FIB) assisted sample preparation

A Hitachi NB Vision 5000, dual-beam FIB/SEM was used to prepare TEM samples from regions of interest. In situ, gallium-assisted tungsten deposition was performed on an area approximately 2 μm × 10 μm; the tungsten layer was 2 μm thick. A 40 kV Ga ion beam with a final beam current of 3 nA and pixel step size of 60 nm was used to remove a 2 × 10 μm lamella from the bulk sample. The unpolished lamella was secured onto a five-post, copper FIB lift-out grid made by Omniprobe. A 10 kV Ga ion beam with a beam current of 10 pA and pixel step size of 3 nm was used to perform final polishing/thinning of the lamella. The approximate thickness of the final lamella was around 100 nm (Eslahpazir et al., 2011).

FIB samples were examined in a JEOL 2010 TEM, equipped with an EDX detector, and operated at 200 kV. Bright field (BF) and dark field (DF) imaging, and X-ray microanalysis were used to characterize kerogen sections.

3.2.10 X-ray photoelectron spectroscopy (XPS)

X-ray photoelectron spectroscopy (XPS) was performed with an AXIS 165 spectrometer (Kratos Analytical) to study the chemical states of the surface

species on kerogen. During XPS analysis, the base pressure in the analytical chamber was lower than 5×10^{-8} Pa and the working pressure was better than 3×10^{-7} Pa. A monochromatic Al Kα (hν = 1486.6 eV) source operating at 210 W was used. The analyzer was operated in fixed analyzer transmission (FAT) mode. High-resolution XPS spectra were obtained at a pass-energy of 20 eV with a step of 0.1 eV. The analyzed spot size was 500×400 μm^2. The binding energy of C 1s in hydrocarbon at 284.8 eV was used to calibrate the binding energy peaks.

3.2.11 Microscopic organic petrology

The sediment samples were placed in 3 cm diameter Teflon molds and then impregnated with a cold-setting EPOTECH® epoxy–resin mixture. After mounting, the molds were polished using carborundum grit and then on a silk-covered lap using alumina-alcohol slurries for the final sample preparation.

Organic petrography was conducted using an incident light Zeiss Axioplan II microscope system equipped with white and fluorescent light sources, a J & M® photometer and a spectrometer (300-1100 nm). Oil-immersion objectives of various magnifications were used to assist in organic matter characterizations (total magnification ranging from 100× to 2500×). A Zeiss Ultraviolet G 365 nm excitation filter (395 nm beam splitter, 420 nm barrier filter) was used. Digital images were captured using Zeiss Axiocam® and Axiovision® software (Sanei et al., 2005).

Relative fluorescence intensity measurements of liptinite macerals (sporinites and alginites) were made at 2.5 nm intervals (420-720 nm). An epiplan-neofluor 40×

water immersion objective (N.A. = 0.95), an ultraviolet G 365 nm excitation filter, a 395 nm beam splitter and a 420 nm barrier filter (HBO 100 W Hg UV-light source) were used during spectral analysis. A black body curve was used to correct spectra for background. A standard tungsten lamp (3100 K) was used as a reference radiator during background correction.

4 Results and Discussion

4.1 Starting samples

The oil sands geological end members from Syncrude's North Mine and Aurora Mine were analyzed by standard Dean-Stark extraction (Bulmer and Starr, 1979) to determine the bitumen, solids and water contents (Table 4-1).

Table 4-1 Bitumen, solids and water contents in oil sands geological end members from Syncrude's North Mine and Aurora Mine.

	Sample	Bitumen (wt %)	Solids (wt %)	Water (wt %)
North Mine	ES	16.6	82.1	1.3
	EC	0.5	94.3	5.2
	MS	8.1	90.6	1.3
	MC	3.4	90.7	5.9
Aurora Mine	ES	9.3	87.3	3.0
	EC	0.1	96.2	3.9
	MS	8.7	86.4	4.2
	MC	1.2	92.9	6.4

The compositions are quite different in these geological end members. The sand samples have higher bitumen content than the clay samples, while the clay samples bear more water. Estuarine sand tends to contain the most bitumen of the geological end members, while estuarine clay has very little bitumen. The

bitumen content difference between marine sand and marine clay samples is not as great as that for estuarine sand and estuarine clay. As is well known, estuarine clay is usually grey and pale in color, while the marine clay is dark. The darkness of marine clay could partially be due to the higher bitumen content. In addition to the heterogeneity for the different geological end members from the same mine site, the same geological end members from the different mine sites (North Mine and Aurora Mine) were also different.

4.2Clay identification and mineralogy analysis

After bitumen removal by Dean-Stark extraction, the bitumen-free solids were prepared by two methods: random preparation and oriented preparation, as described in Section 3.2.1, for XRD analysis. For clay identification, a comparison of XRD patterns for marine clay and estuarine clay samples from the Aurora Mine is shown in Figure 4-1.The samples were first dispersed in water and centrifuged at 6500 rpm for 3 minutes. After centrifugation, 2 mL of supernatant was placed on a glass slide and then dried at 54% RH (saturated $Mg(NO_3)_2$ solution).

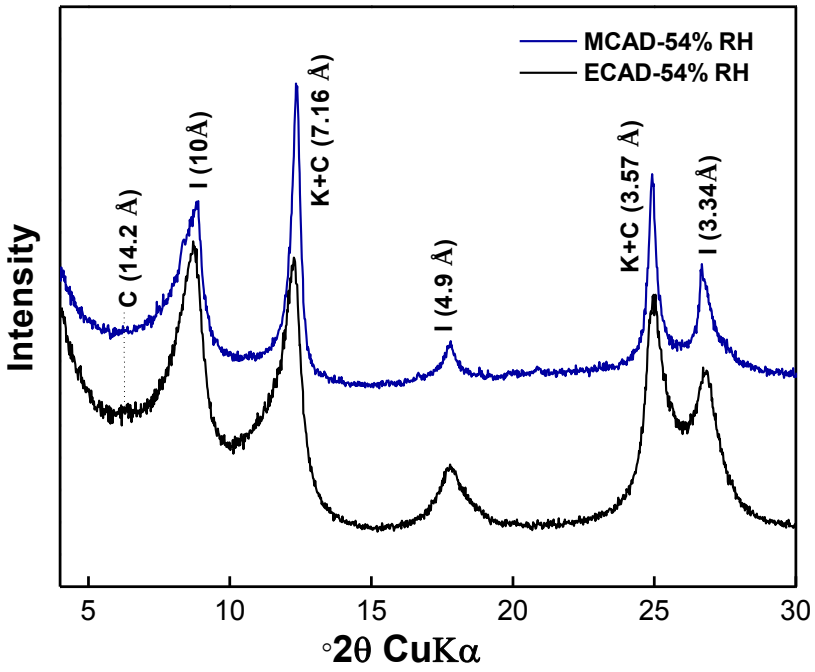

Figure 4-1 XRD patterns for oriented clay samples. I-illite, K-kaolinite, C-chlorite.

Illite and kaolinite are the main minerals in the XRD patterns for all samples as documented by the appearance of reflections with d = 1 nm, 0.49 nm and 0.334 nm (illite) and d = 0.716 nm and 0.357 nm (kaolinite), respectively. From the above comparison, estuarine clay samples had more illite than marine clay.

Expandable clays cannot be identified in air dried (54% RH) samples, due to overlapping of characteristic XRD peaks for smectite and illite at around 1 nm. To distinguish smectite from illite peaks, the air dried samples were ethylene glycol treated at 60°C overnight prior to XRD analysis. Patterns are compared in Figure 4-2.

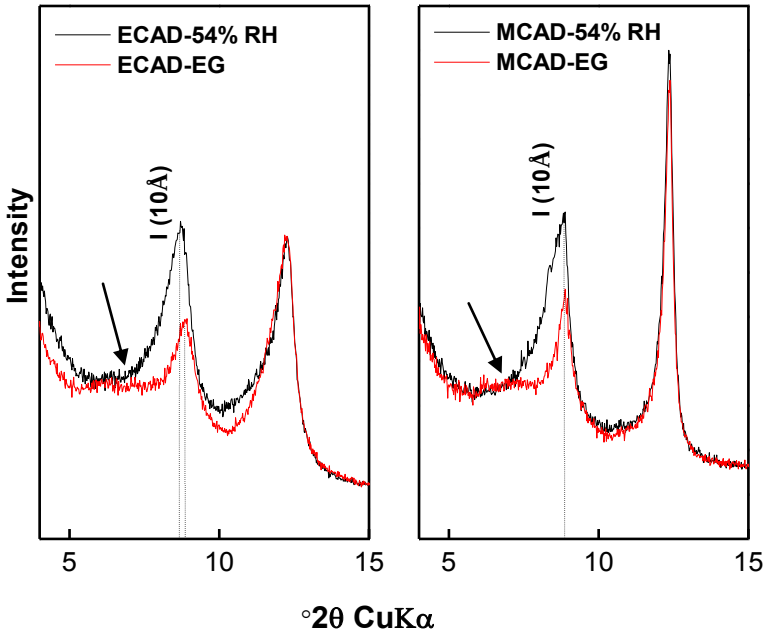

Figure 4-2 XRD patterns for oriented samples after ethylene glycol saturation.

The North Mine end members <0.2μm were analyzed by Osacky et al. (2013). The peak at d spacing of 1.0 nm decreased and there was an extra illite-smectite peak in the larger d spacing region, around 1.2 nm. From the comparison of our samples before and after ethylene glycol treatment, we can see the peak at d spacing of 1.0nm also decreases. There is a very broad peak in the larger d spacing area, as indicated by the arrows. This may be because of the limited amount of expandable clays in the <2μm fraction, or that the method used here is not sufficient to induce clay expansion (Mosser-Ruck et al., 2005).

Randomly prepared powder samples with corundum as the standard were subjected to XRD analysis. The data were extracted by Jade software to Excel.

The data were further used in the RockJock program and the mineral compositions were obtained as shown in Table 4-2.

Table 4-2 Mineralogical composition of geological end members in North Mine (NM) and Aurora Mine (AM) sites (wt%).

	End member	**Quartz**	**K-feldspar**	**Carbonate**	**Pyrite**	**TiO_2 minerals**	**1:1 clay**	**Total 2:1 clays**
NM	ESAD	94.5	3.6	0.2	0.0	0.0	0.8	0.9
	ECAD	52.3	2.7	3.3	0.0	0.7	14.4	26.6
	MSAD	87	3.7	2.5	0.2	0.2	4.1	2.5
	MCAD	72.2	3.9	7.0	0.1	0.3	8.9	7.7
AM	ESAD	78.6	3.2	1.0	0.1	0.0	6.8	10.4
	ECAD	45.3	1.6	0.8	0.5	0.2	21.3	30.7
	MSAD	92.2	2.0	0.5	0.1	0.0	3.0	2.3
	MCAD	58.8	5.1	2.8	0.3	0.0	11.8	21.5

The 1:1 clay is kaolinite in Table 4-2. The total of 2:1 clays is the sum of illite, illite-smectite and chlorite. From the comparison of end members for the two mining sites, it is evident that estuarine sand from the Aurora Mine has a much higher clay content (17.2 wt%) and carbonate content (1.0 wt%) than that from the North Mine (1.7 wt% and 0.2 wt%, respectively). The high clay content or fines content (<45μm) could be one indication of low bitumen content in this sample. Pyrite was not detected in estuarine samples from the North Mine, but showed in estuarine samples from the Aurora Mine. A model of pyrite formation

was proposed by Canfield, Lyons and Raiswell (1996), where organic matter associated with the biogenous flux generates pyrite in the water column. The extent of pyrite formation is limited either by microbial sulfide or by the availability of reactive iron minerals. The terrestrial sediments notably lack reactive iron (Raiswell and Canfield, 1998). Therefore, the estuarine samples from the North Mine are likely formed from continental environment.

4.3Geochemical analysis of geological end members

The fines contents (<45 μm) in the solid residues from both the North Mine and Aurora Mine after the Dean-Stark procedure were determined by wet sieving. Fines and bitumen contents are shown in Table 4-3. Bitumen content is plotted against fines content in Figure 4-3.

Table 4-3 Bitumen and fines contents in the geological end members (wt%).

	North Mine		**Aurora Mine**	
Sample	Bitumen Content	Fines (<45μm) after Dean-Stark	Bitumen Content	Fines (<45μm) after Dean-Stark
ES	16.6	2.0	9.3	20.8
EC	0.5	89.3	0.1	94.4
MS	8.1	19.1	8.7	15.8
MC	3.4	66.6	1.2	92.8

As shown in Table 4-3, the bitumen content in the different geological end members varies significantly. The estuarine sand sample from the North Mine contains 16.6 wt% bitumen, while the estuarine sand sample from the Aurora Mine contains 9.2 wt% bitumen. The large discrepancy between the two samples may be caused by the difference in the fines content. It has been established for the Alberta oil sands that the bitumen and fines contents follow an inverse relationship: the more fines (<45 μm) in the sample, the less bitumen in the oil sands. This is also seen in Figure 4-3. It is known that, the more fines in the sediment, the lower the permeability, therefore, bitumen is less likely to penetrate into it. It can also be interpreted in another way: bitumen migrated from the source rock by various forces and became trapped in the reservoirs in the McMurray Formation. The higher the permeability in the formation end member, the more bitumen can penetrate into it.

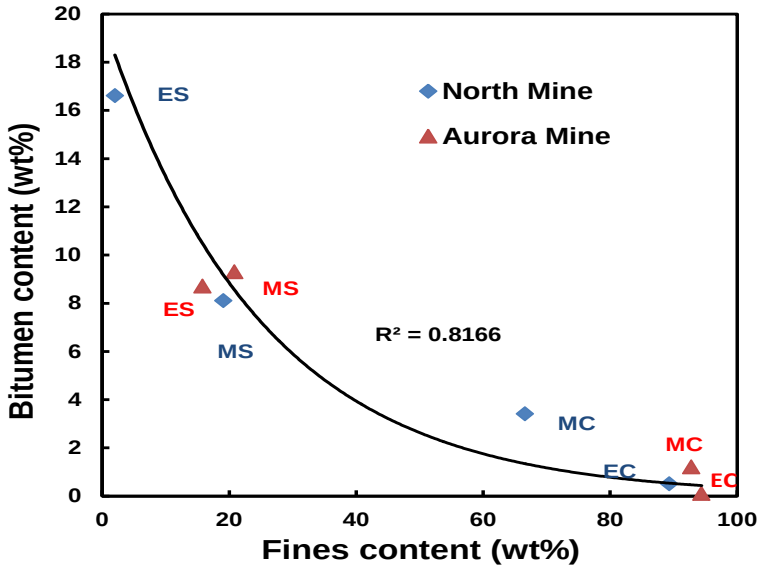

Figure 4-3 Bitumen content versus fines content in the different oil sands geological end members.

After Dean-Stark treatment, which removed soluble bitumen, the clay samples contained more residual organics (total organic carbon, TOC) than their sand counterparts, Table 4-4 and Figure 4-4.

Two methods were used to determine the TOC content, shown in Table 4-4, mainly to observe the difference between the standard TOC method and Rock-Eval analysis. It turns out that the results are more or less the same, so both methods were reliable.

The kerogen content was calculated by the total organic carbon content in end members and carbon content in kerogen, which was determined in Table 4-7. The kerogen content in oil sands end members varied from 1 wt% to 4.6 wt%. In clay samples, the kerogen content was larger than bitumen content, shown in Table 4-3.

Table 4-4 Total organic carbon and total nitrogen contents of different oil sands end members in the Aurora Mine deposit.

	Dry Combustion Method			**Rock-Eval Method**	
	Costech 4010 analyzer after H_2SO_3 treatment			Rock-Eval 6	Vario Micro Cube
Sample*	TN (wt%)	TOC (wt%)	Kerogen (wt%)	TN (wt%)	TOC (wt%)
ESAD	0.02	0.73	0.99	0.032	0.8
ECAD	0.05	1.34	1.81	0.05	1.04
MSAD	0.04	0.96	1.28	0.036	0.89
MCAD	0.09	3.40	4.61	0.085	2.98

***** The suffix "AD" in the sample name stands for "after Dean-Stark".

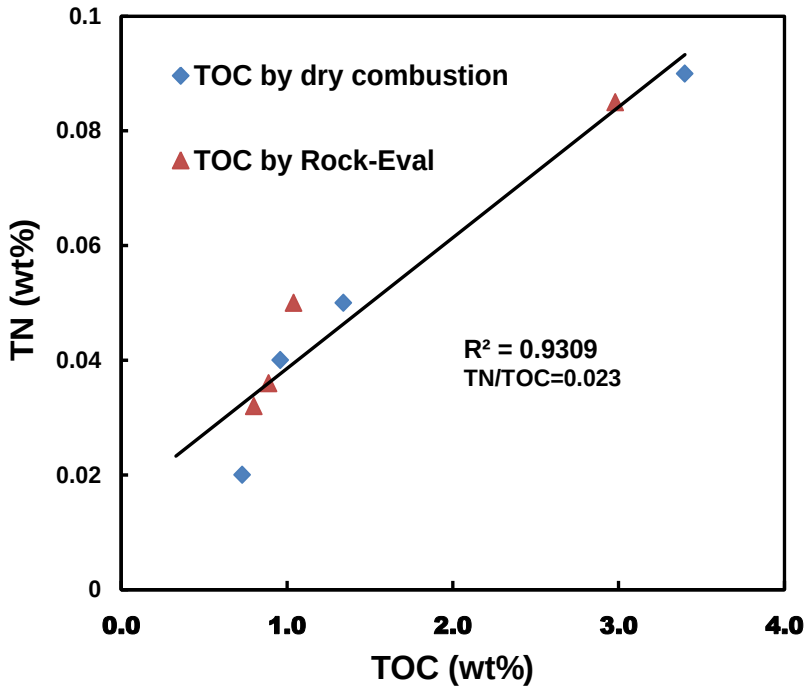

Figure 4-4 TN versus TOC in Aurora Mine geological end members after Dean-Stark treatment.

Figure 4-4 shows that the total nitrogen (TN) content is linearly correlated to the total organic carbon (TOC) in the solid residues of Dean-Stark treated Aurora Mine samples. The ratio of total nitrogen to total organic carbon (i.e., the slope of the straight line) is about 0.023, while in the corresponding bitumens, the ratios of TN/TOC are less than 0.014, in Table 4-7. This implies that the nitrogen content is higher in kerogen than in bitumen.

Earlier research also showed that the TOC content increased in the fine size fractions of bitumen-free solids (Osacky et al., 2013). Because clay minerals constitute the solids fraction with the largest surface area in these samples, it is

reasonable to infer that the toluene insoluble organic matter, i.e., kerogen, in the different geological end members is mostly adsorbed on clay minerals.

4.4 Kerogen types and maturity

Geochemical characterization of the geological end members from the North Mine and Aurora Mine was conducted by Rock-Eval 6 (Vinci Technologies, France), and the results are listed in Table 4-5. It has been proposed that when T_{max} = 400ºC-435ºC, the sample is "immature" and still has hydrocarbon generating potential. T_{max} = 435ºC-470ºC represents the mature or oil zone and T_{max} > 470ºC represents the postmature zone (Peters and Cassa, 1994), where there is no potential for oil and gas formation. Kerogen can also be classified into three types based on the Modified van Krevelen diagram, which plots hydrogen index (HI) against oxygen index (OI). S1, S2, S3, pyrolysable carbon (PC) and residual carbon (RC) were obtained during Rock-Eval analysis. HI and OI were calculated from Rock-Eval data as described in Section 2.4.2 and are listed in Table 4-5. As can be seen, the HI in the marine samples was generally higher than that in the estuarine samples and the OI in the marine samples was lower than that in the estuarine samples. The reason is that the marine organisms and algae, in general, are composed of lipid-rich and protein-rich organic matter, where the ratio of H to C is higher and the O to C ratio is lower than in the carbohydrate-rich constituents and polysacharride-rich remains of land plants. Another observation is that, the HI in the North Mine was higher than the HI in the Aurora Mine; this may indicate the Aurora Mine sediments are older than the North Mine sediments.

Table 4-5 Geochemical analysis of different oil sand end members analyzed by Rock-Eval 6.

	End members*	**S1**	**S2**	**S3**	**T_{max} (ºC)**	**PC (%)**	**RC (%)**	**TOC (%)**	**HI**	**OI**
North Mine	ESAD	0.32	1.33	0.34	403	0.16	0.25	0.41	324	83
	ECAD	0.35	1.83	1.70	423	0.25	1.01	1.26	145	135
	MSAD	0.36	2.41	0.42	427	0.26	0.83	1.09	221	39
	MCAD	0.44	5.35	0.64	429	0.53	1.91	2.44	219	26
Aurora Mine	ESAD	0.09	0.86	0.54	421	0.12	0.68	0.80	108	68
	ECAD	0.03	0.64	0.86	425	0.10	0.94	1.04	62	83
	MSAD	0.08	0.91	0.39	422	0.12	0.77	0.89	102	44
	MCAD	0.22	2.97	0.78	424	0.33	2.65	2.98	100	26

* The suffix "AD" in the sample name stands for "after Dean-Stark".

In Table 4-5, the solid residues (from Dean-Stark) from both the North Mine and Aurora Mine showed a T_{max} of <435ºC (varying from 403ºC to 429ºC). Generally, the result can be interpreted as all the kerogens are immature but close to mature, meaning the kerogens still have some potential to generate oil and gas.

From the HI and OI, the Modified van Krevelen diagram was plotted (Figure 4-5 and Figure 4-6). As can be seen, the kerogens from different geological end members were between type II and III. The marine samples have more type II kerogens, while estuarine samples have more type III kerogens. It has been

reported (Peters and Moldowan, 1993) that the maceral groups in different types of kerogen were different: most of the type II kerogens were liptinite and originated from planktonic debris, spores and algae, while type III kerogens were mainly vitrinite, and originated mostly from land plants. Because of different occurrences and maturities of kerogen in estuarine and marine sediments, the bitumen and solvent retention capability could be different during a non-aqueous bitumen extraction process.

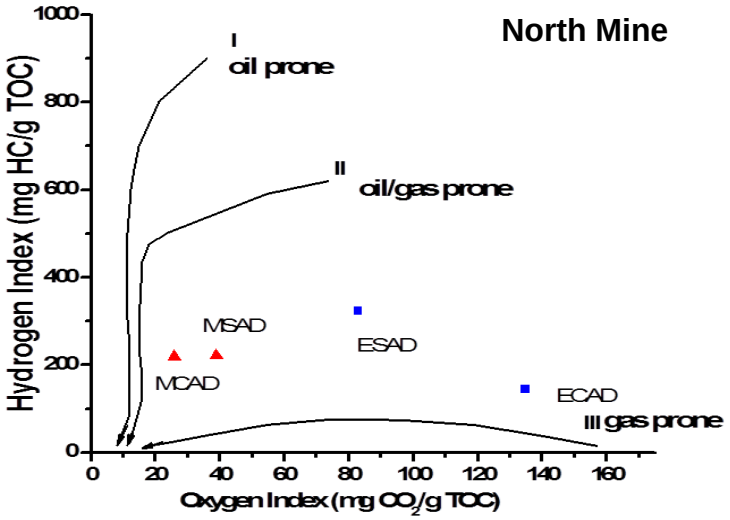

Figure 4-5 Modified van Krevelen diagram for the North Mine geological end members.

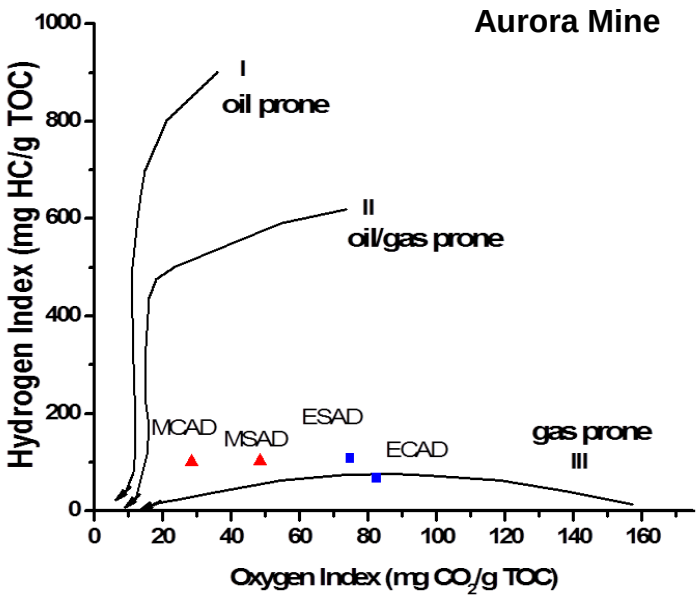

Figure 4-6 Modified van Krevelen diagram for the Aurora Mine geological end members.

One circumstance that needs to be emphasized is that the bitumen in the oil sands sediments does not originate from the sediment in which it exists, due to bitumen migration. In other words, the geological end members on the surface are not the source rock that generated bitumen, but bitumen traps or reservoirs. Even after bitumen extraction, it is almost certain that there still remains some amount of un-extractable bitumen that is retained by the kerogen network and adsorbed on the mineral matrix. Therefore, the kerogens studied here are mixed with a finite amount of bitumen.

4.5 Chemical composition of isolated kerogens and their impurities content

The solid residues from the Aurora Mine after Dean-Stark extraction were subjected to HCl/HF digestion, detailed in Section 3.2.4, to remove inorganic mineral matter, leaving kerogen in the residue with an intact morphology. After

acid digestion, a black and dark gray mass was obtained. It was subjected to elemental analysis by several methods, namely a CHNS elemental analyzer and XRF, and sulfur content was used to calibrate the amount of heavy elements.

Table 4-6 Elemental analysis of isolated kerogen from the Aurora Mine (wt%).

	N	**C**	**H**	**S**	**O**	**Mg**	**Al**	**K**	**Ca**	**Fe**	**Zr**	**Ti**
K-ESAD	0.87	45.68	3.05	9.65	15.54	0.67	0.67	9.74	0.04	7.31	0.34	0.17
K-ECAD	0.87	38.20	2.77	3.87	18.38	2.41	4.77	1.43	0.29	2.55	0.47	0.75
K-MSAD	0.92	44.88	2.63	10.73	14.57	1.18	1.19	10.91	0.11	9.22	0.39	0.25
K-MCAD	1.13	51.56	2.93	6.56	15.16	2.95	2.69	1.08	0.18	3.96	0.31	0.20

The results of elemental analysis are listed in Table 4-6. As can be seen from Table 4-6, after the HCl/HF digestion, the resulting kerogen samples still seem to contain significant amounts of mineral matter. In fact, SEM/EDX results show that various mineral grains are still present in the acid digestion residues, Figure 4-7. In the SEM BSE image, Figure 4-7, the bright regions with various sizes contain S, Fe, Al, Ti, Zr, etc., possibly resulting from FeS_2 (pyrite), TiO_2 minerals (anatase and brookite), zircon and fluorides.

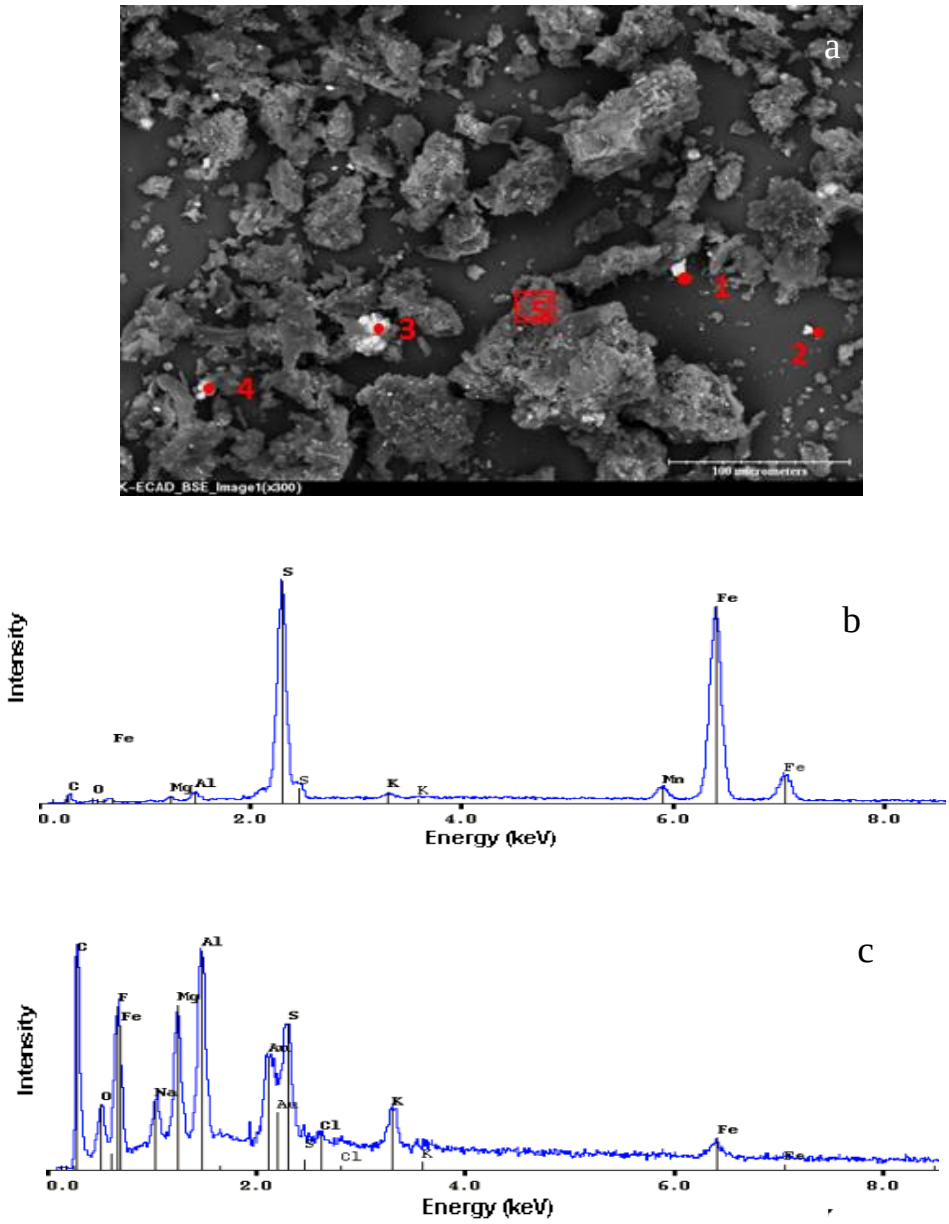

Figure 4-7 SEM/EDX analysis of impurities in K-ECAD. A - BSE image of kerogen sample K-ECAD; b - EDX spectrum from point 1 (the spectra from points 2, 3 and 4 are similar); c - EDX spectrum from area 5.

Higher atomic number elements will show up brighter than lighter elements in BSE images. However, the samples were gold coated to avoid carbon analysis in the kerogens, which made it difficult to distinguish the heavy elements. Several points (points 1-4 in Figure 4-7a) were chosen randomly and analyzed by EDX,

which showed that the bright regions are most likely pyrite (Figure 4-7b). A significant amount of pyrite was left in the kerogen after acid treatment. Area 5, in Figure 4-7a, was chosen for EDX analysis. A large amount of F was present (Figure 4-7c). During acid treatment of the minerals, fluorides may have been formed as by-products (Durand, 1980).

In addition to pyrite and fluorides, other heavy elements (e.g., Ti and Zr) were also detected by EDX elemental mapping (Figure 4-8). An example of one area is shown in Figure 4-9a.

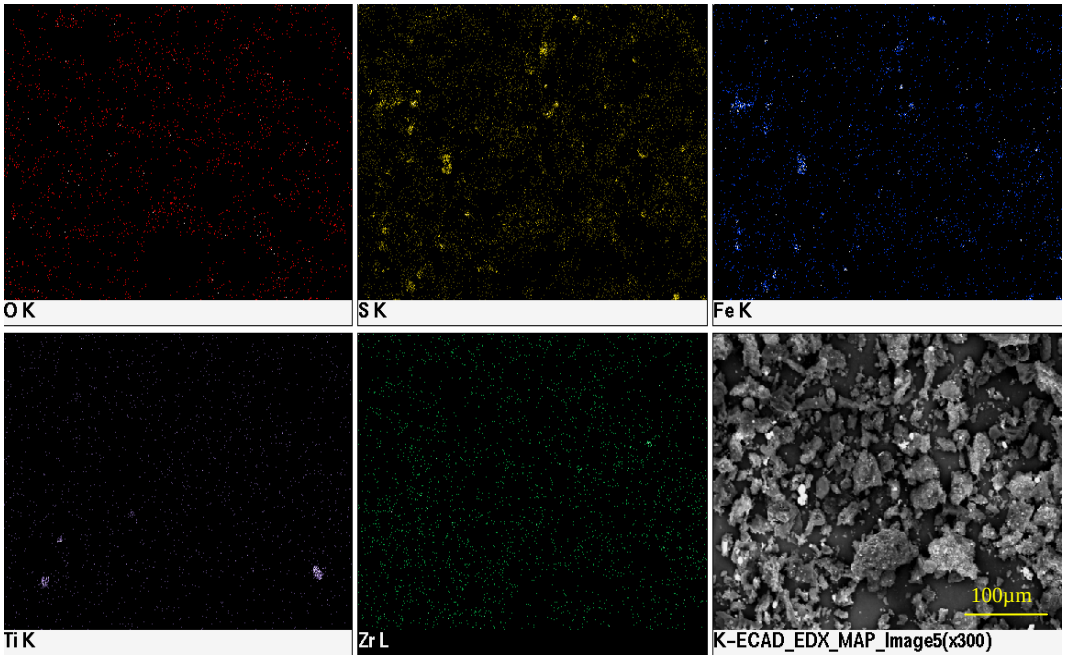

Figure 4-8 EDX elemental mapping of kerogen in K-ECAD.

These maps took about three minutes to collect. Short mapping times were used because the purpose was to locate heavy elements and then analyze them more carefully through EDX spot analysis. EDX spectra were collected from Ti- and

Zr-rich regions in Figure 4-9a; examples are shown in Figure 4-9b and Figure 4-9c).

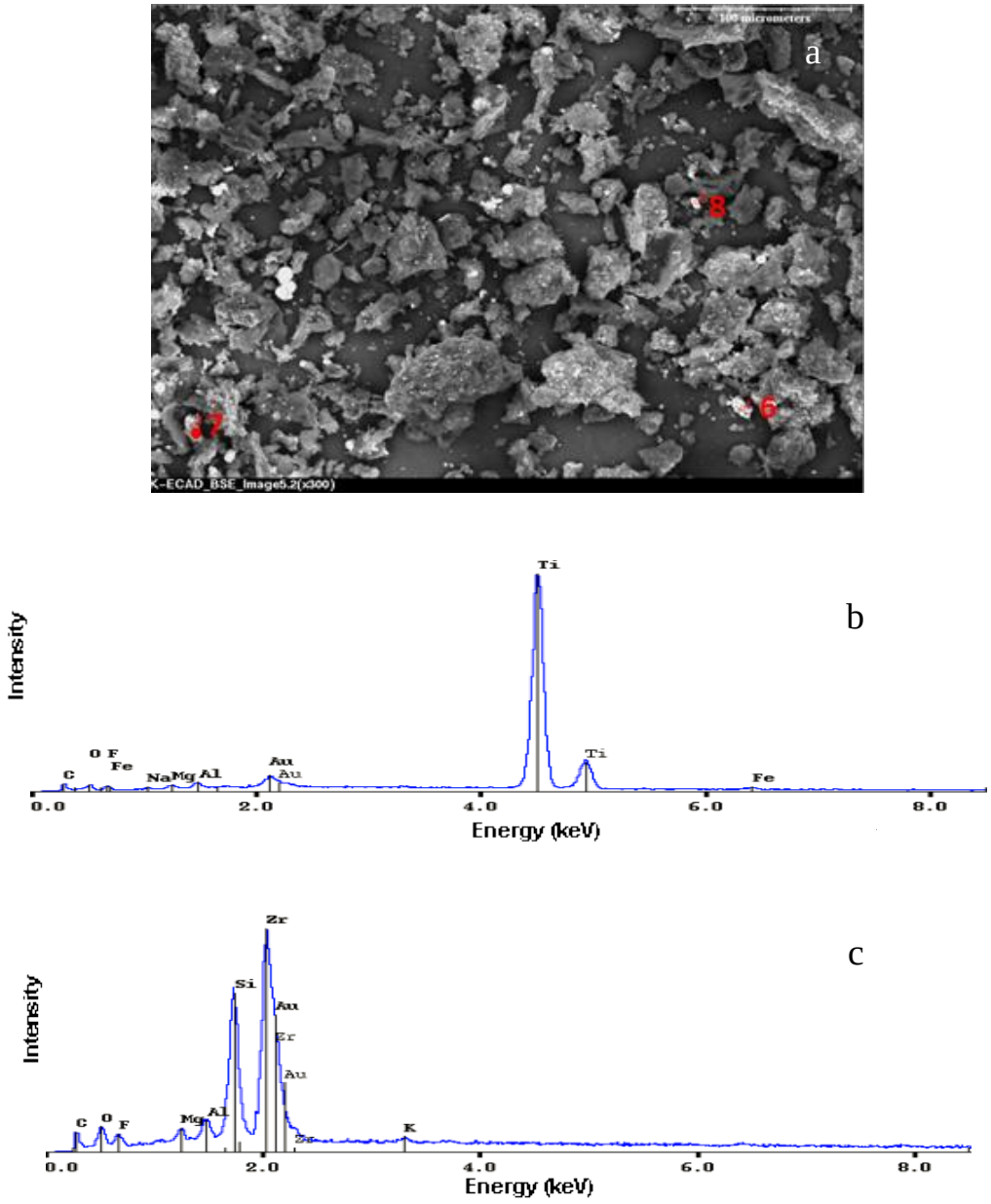

Figure 4-9 SEM/EDX analysis of Ti, Zr in K-ECAD. a - BSE image of kerogen sample K-ECAD; b- EDX spectrum from point 6 (spectrum from point 7 is similar); c-EDX spectrum from point 8.

The spectra in Figure 4-9b and Figure 4-9c show the presence of Ti-rich and Zr/Si-rich regions, respectively, in the kerogen. The presence of minerals in the

isolated kerogen was due to incomplete acid digestion, protection of minerals by organic matter coatings and newly formed by-products.

Although the oxide and silicate minerals are stable and do not contribute to organic analysis, FeS_2 can contribute to S measurement. Under a wet atmosphere during isolation of kerogens, FeS_2 surfaces may also be oxidized into hydrated iron sulphates or oxides. Sulphates can contribute to the sulfur and oxygen analysis. Newly formed fluorides can contribute to oxygen and hydrogen measurement because of water inclusion (Durand, 1980).

To better characterize the kerogen without these interferences, the kerogens were subjected to density separation in a heavy liquid of zinc bromide with 5% HCl. The specific gravity (SG) of the heavy liquid was 1.65. This value was chosen because the densities of almost all types of kerogen are smaller than 1.5 g/cm^3 and those of the minerals are larger than 2.6 g/cm^3.

The purified kerogens after density separation were subjected to CHNSO and XRF analysis. Again, sulfur content obtained from the CHNS analyzer was used to calibrate the heavy element content obtained from XRF. Table 4-7 and Table 4-8 list almost all elements in the kerogens. Fluorine was not detectable in XRF and cannot be obtained by CHNSO elemental analysis. Kerogen content in the purified kerogen samples was approximately 95 wt%. However, there was still 0.4-2 wt% Fe in the purified kerogen sample, possibly due to the close association of FeS_2 with organic matter. Organic sulfur (OS) content in the kerogen samples was calculated by subtracting pyritic sulfur from the total sulfur content.

Elemental analysis of bitumen was also performed by the same methods and the results are compared with the kerogen samples in Table 4-7. It is interesting to note that for the bitumen samples, the total OS was the same as the total sulfur content. Obviously, during the bitumen extraction process, the toluene did not bring any pyrite particles to the extracted bitumen.

Table 4-7 shows that the nitrogen and oxygen contents in the kerogen samples were higher than those in bitumen and that the carbon and hydrogen contents in the kerogen samples were lower than those in bitumen. In the purified kerogen samples, the N/C ratio was approximately 0.019, higher than the N/C ratio in the bitumen extracted from the corresponding oil sands geological end members. The OS was lower in kerogen than that in bitumen, which was somewhat surprising.

Table 4-7 Elemental analysis of kerogen (SG <1.65) and bitumen in different geological end members from the Aurora Mine (wt%)

	N	**C**	**H**	**S**	**O**	**OS**	**N/C**	**OS/C**
K-ESAD-f	1.39	73.75	4.73	5.67	11.68	3.42	0.019	0.046
K-ECAD-f	1.43	73.96	4.48	2.19	14.21	1.79	0.019	0.024
K-MSAD-f	1.44	74.91	4.70	4.76	12.27	2.60	0.019	0.035
K-MCAD-f	1.42	73.77	4.17	2.49	14.79	1.92	0.019	0.026
Bitumen-ES	0.95	84.83	10.03	4.99	2.86	4.99	0.011	0.059
Bitumen-EC	0.67	84.12	9.84	4.44	3.77	4.44	0.008	0.053
Bitumen-MS	1.23	85.01	9.98	5.08	2.82	5.08	0.014	0.060
Bitumen-MC	0.84	85.18	10.21	4.29	3.28	4.29	0.010	0.050

Table 4-8 Heavy elements in kerogen after density separation, analyzed by XRF (wt%)

	Mg	**Al**	**Si**	**K**	**Ca**	**Fe**	**Ti**	**Zr**	**Zn**
K-ESAD-f	0.10	0.22	0.02	0.02	0.02	1.96	0.02	0.03	0.15
K-ECAD-f	0.10	0.28	0.02	0.01	0.05	0.35	0.08	0.03	0.31
K-MSAD-f	0.09	0.18	0.02	0.00	0.02	1.88	0.02	0.03	0.22
K-MCAD-f	0.25	0.25	0.01	0.19	0.06	0.49	0.01	0.03	0.26

There still are some heavy elements present in the kerogen even after density separation, shown in Table 4-8, especially iron, possibly pyrite. Previous studies indicated that pyrite and titanium oxides were surrounded by carbon shells (Oberlin et al., 1980).

Elemental mapping through SEM-EDX was again conducted to see the homogeneity of the kerogen sample. Figure 4-10 is the elemental map for sulfur content in the ECAD-f kerogen after density separation. The left and right images were collected in different areas. The green spots indicate sulfur species in the kerogen. The slight sulfur richness discrepancy in the two areas may be because of the difference in collection time, or there is more sulfur content in area a than area b.

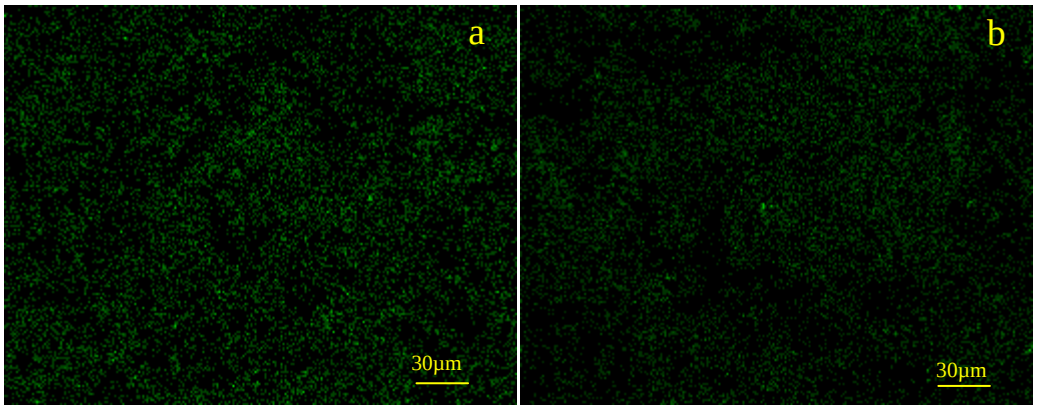

Figure 4-10 Elemental mapping of S in different areas of ECAD-f by SEM/EDX. Green areas indicate sulfur in the kerogen.

Sulfur elemental mapping of different areas after density separation, shown in Figure 4-10, showed higher homogeneity than the sulfur mapping before density separation (Figure 4-8). The mineral grains in kerogens after density separation were finely dispersed. Therefore, kerogen samples after density separation are more suitable for micro sample preparation and analysis.

A pure organic region, located using SEM X-ray mapping, was sectioned and thinned in the FIB instrument (Figure 4-11). Figure 4-11 shows the thinned section detached from the kerogen sample and connected to a probe by means of depositing tungsten. This section was attached to a copper lift-out grid and subsequently polished to a thickness of about 100 nm using FIB.

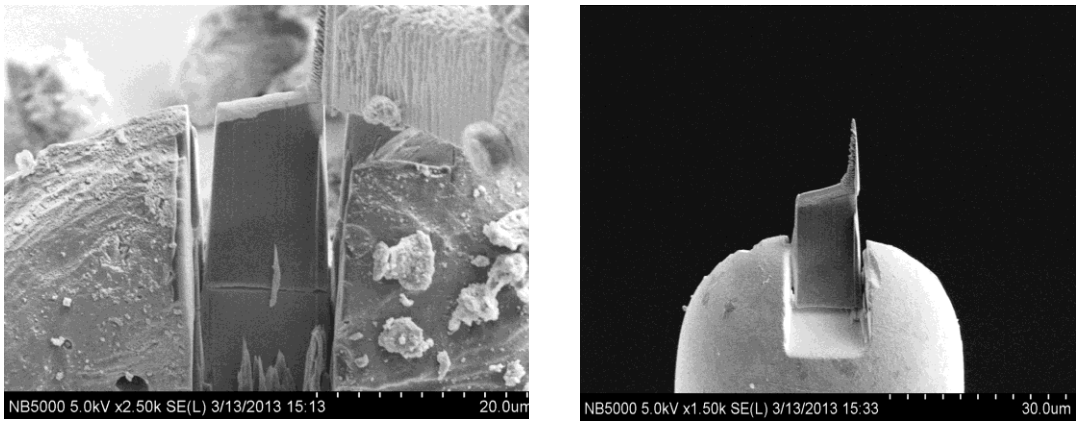

Figure 4-11 FIB preparation of kerogen sample K-MCAD-f for TEM analysis.

The FIB sample was examined in the Philips CM20 TEM equipped with an EDX detector. A TEM bright field (BF) image is shown in Figure 4-12a. Two areas are indicated, as area 1 and area 2, in Figure 4-12a. EDX analysis was performed on these two regions (Figure 4-12b and Figure 4-12c, respectively).

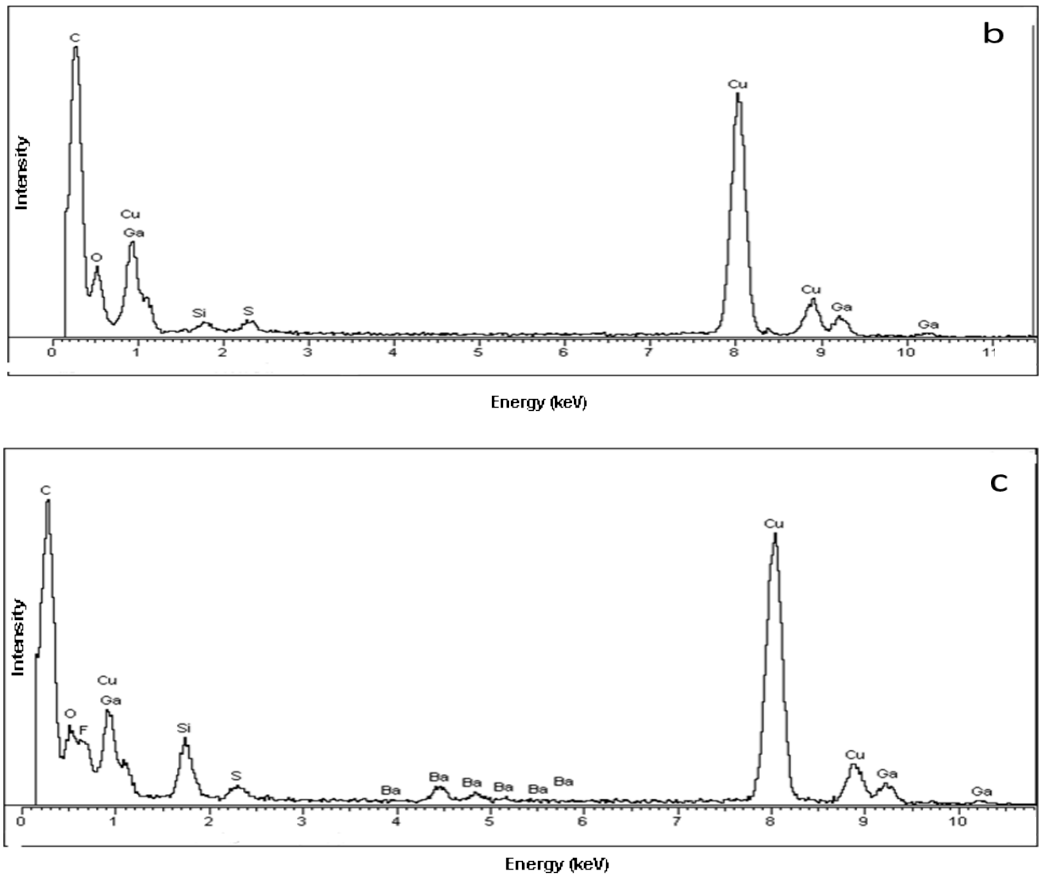

Figure 4-12 TEM/EDX analysis of FIB kerogen sample. a - TEM BF image of FIB sample; b - EDX spectrum of area 1; c - EDX spectrum of area 2.

It can be seen that area 1 is from kerogen and consists of mostly carbon with some oxygen and sulphur, as well as a small amount of silicon. The silicon could be from quartz because of the incomplete acid digestion. The sample before TEM analysis was transferred to a copper finger, which was cut by a gallium beam to create a gap to hold the sample, and the gallium beam was used to mill the surface of the sample to thin it to 100 nm. This gallium milling of the sample for TEM analysis could contaminate the surface of the sample; therefore, the presence of Ga in the kerogen sample was from the Ga beam during the milling of the sample surface. During the TEM analysis of the sample, a beam of electrons was

transmitted through the ultra-thin specimen, interacting with the specimen as it passes through. The Cu X-ray signals in the EDX spectra were because of electrons hitting the Cu finger. Area 2 also shows the same elements, but contains barium, as well as some amount of silicon and fluorine. Other similar regions were observed in the FIB sample. The fluorine and silicon in the nano size region could be due to the newly formed fluorides during kerogen isolation. Other researchers also analyzed the minerals in isolated kerogen. Barium was also found and was attributed to mainly barite, which could not be destroyed or only slightly destroyed (Durand, 1980).

4.6 Sulfur groups in kerogen

As the isolated kerogen generally had a lower ratio of organic sulfur to organic carbon than the original bitumen, XPS was performed to examine whether the sulfur species were the same. The measurements were performed on the purified kerogen (SG <1.65) from estuarine clay and marine clay, as well as on bitumen. XPS analysis of bitumen was performed at the same time. Bitumen was toluene-extracted from a oil sands ore sample, named 3A in the Syncrude sample bank. Sulfur content in the bitumen was 4.77 wt%. The sulfur spectra were scanned over a narrow range and are compared in Figure 4-13. The bitumen used in the XPS analysis was from bulk oil sands to eliminate the possible difference of bitumen contained in individual geological end members. The XPS spectra indicate that it only contained organic sulfur.

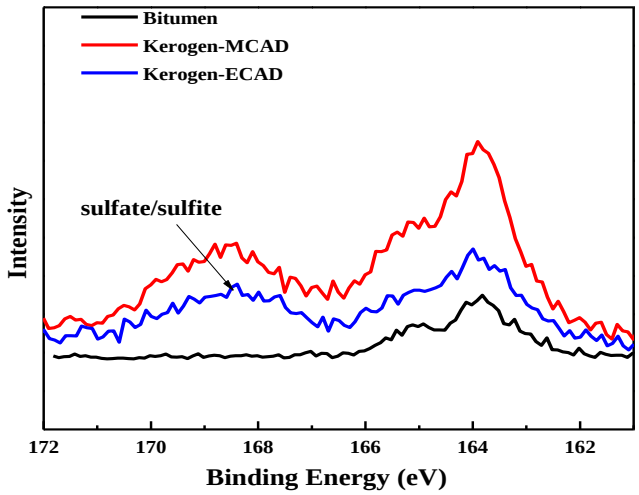

Figure 4-13 XPS spectra showing the S 2p electron binding energies in bitumen and isolated kerogens.

The S 2p binding energy spectra for the kerogens are more complex than that for bitumen and are comprised of two low binding energy peaks (~164 eV and ~165 eV) and a higher binding energy peak (~169 eV). Bitumen only showed the two low binding energy peaks at about 164 eV and 165 eV. The higher binding energy peak at about 169 eV in kerogen is predominantly from sulfate, with possible contributions from lower oxidation valence species such as sulfite and sulfones (Kelemen, 2007), which were not detected in bitumen. The sulfur 2p binding energy peaks are deconvoluted and shown in Figure 4-14. The sulfur 2p spectrum from individual sulfur species are simultaneously deconvoluted using components with fixed energy positions. Individual sulfur species are comprised of 2p3/2 and 2p1/2 components at a 2 to 1 intensity ratio separated by a binding energy of 1.18 eV. In the kerogens, the lower binding energy signal contained contributions from FeS_2 (162.3 ± 0.1 eV), aliphatic sulfur (163.3 ± 0.2 eV), aromatic sulfur (164.1 ±

0.1 eV) and sulfoxide (165.7 ± 0.3 eV) components, each with FWHM values of 1.0 ± 0.2 eV. The higher energy signal was curve-resolved using two components at 167.8 ± 0.1 eV and 168.5 ± 0.1 eV having 2p3/2 and 2p1/2 components of FWHM 1.5 ± 0.1 eV. In bitumen, the lower binding energy signal originated from aliphatic sulfur, aromatic sulfur and sulfoxide.

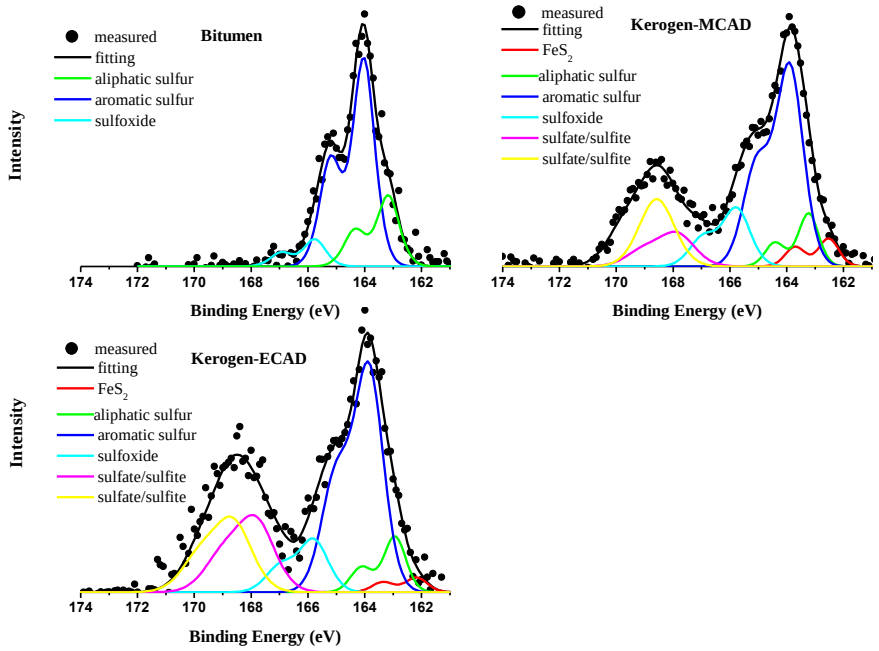

Figure 4-14 Deconvolution of S 2p peaks, from Figure 4-13, in bitumen and the kerogens.

It is clear that the inorganic sulfur species such as pyrite, sulfate and sulfite were not dissolved during the non-aqueous extraction of oil sands bitumen. They were, therefore, associated with the toluene-insoluble organics (kerogen) in the extraction residues.

The XPS spectra of sulfur were simutanuously deconvoluted using the same fixed energy positions as described above, developed by Kelemen et al. (2007). The lower energy sulfur peaks of both marine and estuarine kerogens can be deconvoluted into four sulfur species. As can be seen, the sulfur in kerogens from marine clay and estuarine clay did not appear to be different. In Kelemen et al.'s studies (2007), the lower sulfur peaks of some kinds of kerogens were comprised of only two or three sulfur species.

Samples of marine clay, estuarine clay and marine sand after bitumen extraction were examined using white and fluorescent light microscopy. Figure 4-15a and Figure 4-15b show images of the marine clay sample with white light (left hand side) and fluorescence light (right hand side). In marine clay, the quartz particles are indicated and marked by yellow lines in Figure 4-15, most of which are 15 μm to 25 μm in length. The brown areas are kerogen, which is transparent brown in white light, but fluoresces red or blue in fluorescent light (Sanei et al., 2005). The different fluorescing colors could be from different types and evolution stages of kerogen, referred to as maturity. In Figure 4-15b, it can be seen that there are a lot of black regions which are still dark under fluorescence light conditions. These regions are also organic matter, most likely bitumen.

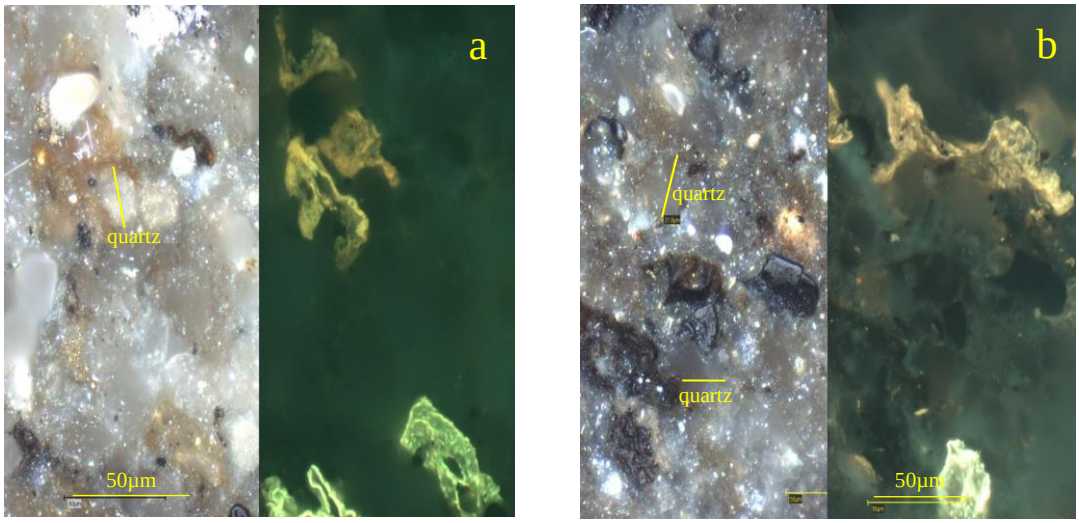

Figure 4-15 Transmission optical imagesof marine clay (MC) using white (left) and fluorescence (right) light microscopy. a - area 1 of MC sample imaged with microscopy; b – area 2 of MC sample imaged with microscopy.

Estuarine clay samples were also examined with fluorescence light (Figure 4-16). Different types of kerogen were detected. The kerogen in Figure 4-16a is spongy, while in Figure 4-16b the kerogen is flaky. The different structures of kerogen may be a result of the different origins of kerogen.

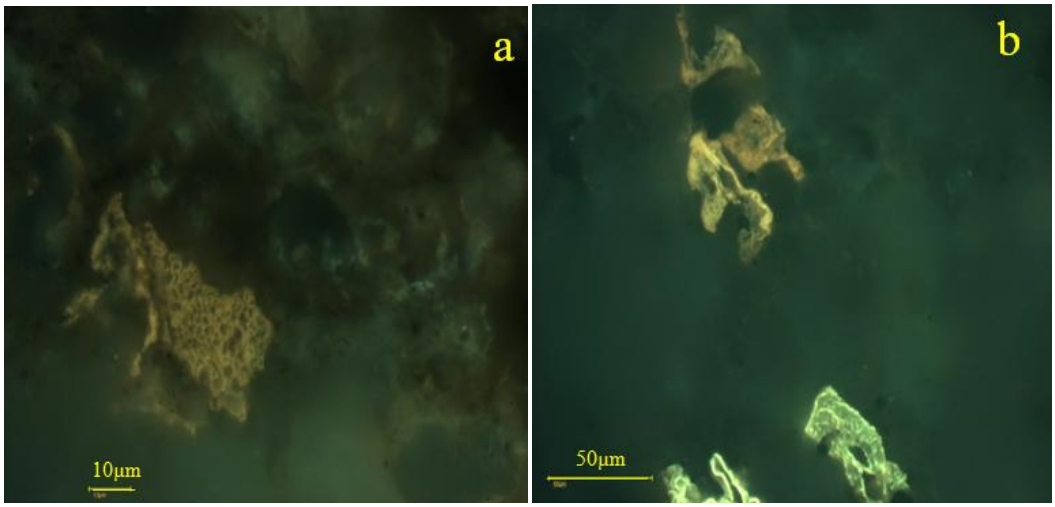

Figure 4-16 Estuarine clay (EC) sample images in fluorescence microscopy. a - area 1 of EC sample imaged with fluorescence microscopy; b – area 2 of EC sample imaged with fluorescence microscopy.

Figure 4-17 shows images for the marine sand sample under white and fluorescence light microscopy conditions.

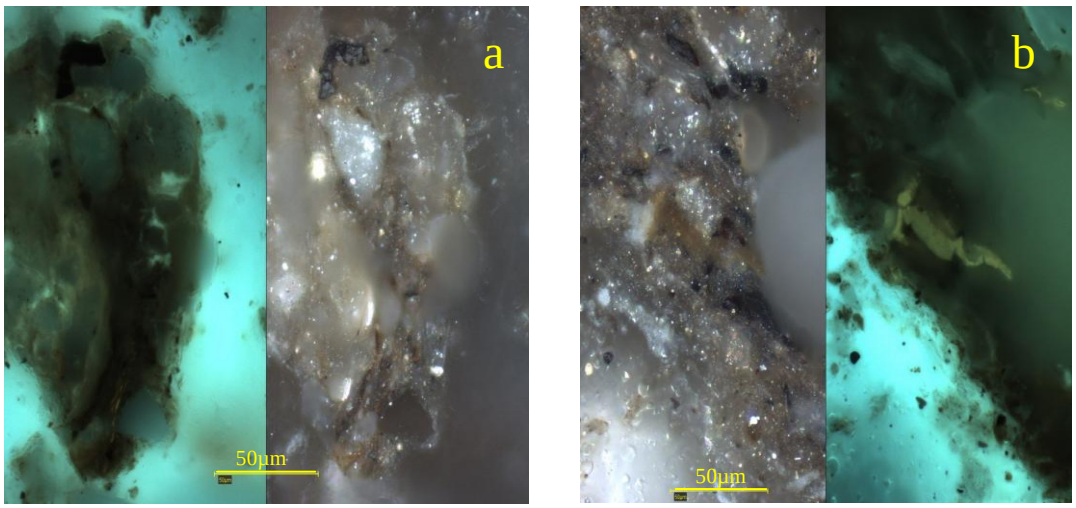

Figure 4-17 Transmission optical images of marine sand after Dean-Stark extraction (MSAD) using white (left) and fluorescence (right) light microscopy. a - area 1 of MSAD sample imaged with microscopy; b - area 2 of MSAD sample imaged with microscopy.

Through extensive examination, it can be seen that kerogen in the MSAD sample seems to lose its fluorescence, although a minor amount of fluorescing kerogen still exists in the sample.

A large amount of pyrite was observed, which was closely associated with organic matter (Figure 4-18) in the marine clay sample. In isolated kerogen, pyrite is the main impurity. Pyrite, which is golden in color, is usually present around organic matter. This can be explained by the formation process for pyrite.

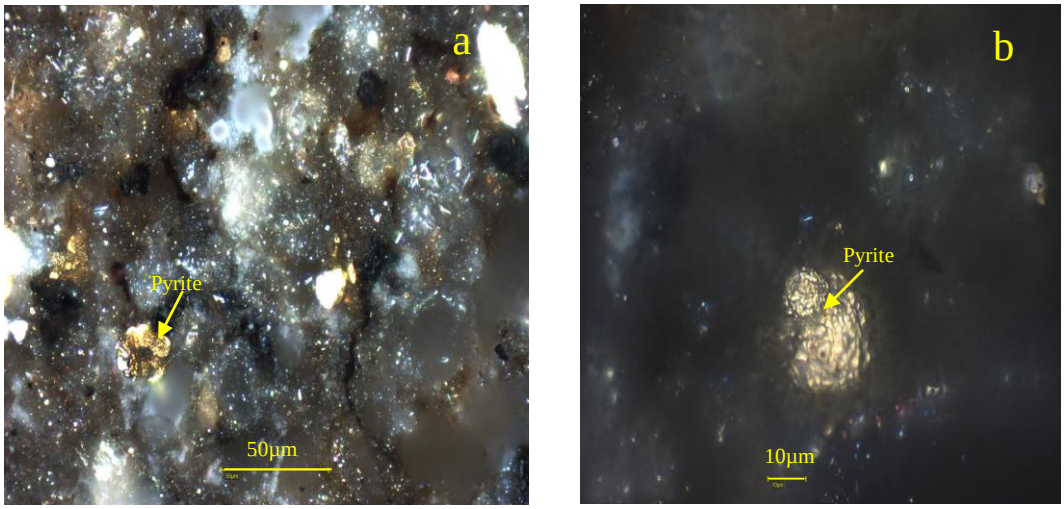

Figure 4-18 Pyrite associated with organics examined through white light microscopy in marine clay (MC) sample. a - area 1 of MC sample under light microscopy, scale 50μm, golden grains are areas are pyrite, organic matter are the black or light brown areas ; b – area 2 of MC sample imaged with light microscopy, scale 50μm. The round, golden region is pyrite.

In the process of organic matter decomposition, SO_4^{2-} acts as alternative electron acceptor during oxidation of organic matter by bacteria, e.g., $SO_4^{2-} + 2H^+ + 2(CH_2O) \rightarrow 2CO_2 + H_2S + 2H_2O$. H_2S originates from bacterial activity. In the presence of ferrous ions, pyrite can form (Berner, 1970; Schoonen, 2004).

$$\text{organic} + SO_4^{2-} \xrightarrow{\text{bacteria}} H_2S \xrightarrow{Fe^{2+}} FeS \xrightarrow{H_2S} FeS_2$$

In summary, there are significant amounts of kerogen and soluble organics (bitumen, coal, etc.) in oil sand end members. After Dean-Stark extraction, there is still a certain amount of residual bitumen retained by the mineral matrix and kerogen network. Pyrite, which is always associated with organics, can also be observed through microscopic observation. The in-situ formation of pyrite during

the bacterial oxidation of the hydrocarbon is the main reason for the close association of pyrite with kerogen.

5 Conclusions and Future Work

5.1 Summary and conclusions

1. Oil sands samples from estuarine and marine ores of Syncrude Canada's North Mine and Aurora Mine were collected. Clays and sands were separated manually; therefore, four oil sands geological end members were obtained as test samples from each mine: estuarine sand (ES), estuarine clay (EC), marine sand (MS), marine clay (MC).

2. Estuarine clay and marine clay samples were analyzed by optical microscopy. Kerogen can be directly and clearly observed through fluorescent microscopy. There is a significant amount of kerogens and soluble organics (bitumen, coal, etc.) in the oil sands end members.

3. The four geological end members from each mine were subjected to the Dean-Stark process and all the bitumen was considered to have been removed. The bitumen content and fines content in each of the geological end members were determined. This work confirmed the inverse correlation between the fines content (<45 μm material) and bitumen content.

4. The bitumen-free geological end members were subjected to quantitative XRD analysis for mineralogical determination with the assistance of the RockJock program. Also, oriented samples were prepared to indentify the types of clays in the samples.

5. Compared to previous analyses conducted by Osacky et al. (2013) on the North Mine samples, in the Aurora Mine petrological end members, expandable clays also exist, but the new generated peaks in large d-space areas are very broad and hard to see because of their low intensity. The <2 μm samples we used either contained a limited amount of expandable clay or the vapor ethylene glycol treatment was insufficient to induce expandability.

6. Quantitative XRD analysis indicated that the estuarine sand from the Aurora Mine had a much higher clay content (17.2 wt%) and carbonate content (1.0 wt%) than that from the North Mine (1.7 wt% and 0.2 wt%, respectively). The high clay or fines content (<45μm) was consistent with a low bitumen content in this sample.

7. The nitrogen content was measured to estimate the amount of toluene insoluble organic matter, kerogen, in bitumen-free oil sands end member samples. The solid residues after Dean-Stark treatment for all four geological end members from the Aurora Mine had similar nitrogen to carbon (N/C) ratios of 0.023, which was higher than the ratio in the corresponding bitumen, which was less than 0.014 This relatively high N/C ratio signifies the presence of kerogen. The kerogen content in oil sands geological end members ranged from 1 wt% to 4.6 wt%.

8. The kerogen types were determined in the geological end members by Rock-Eval 6. It was observed that the kerogens were all immature. Therefore the oil sands source rock still has hydrocarbon generating potential. The types of kerogen from the different geological end members were between type II and type III, with

more type III kerogens in estuarine samples and more type II kerogens in marine samples. Because of the high oxygen and low hydrogen contents in estuarine kerogens, they are not suitable for oil production.

9. The kerogens were isolated and purified from the solid residues by HCl/HF treatment and heavy liquid separation. The isolated kerogens showed much higher N and O contents than the corresponding bitumen. While the kerogens contained both organic and inorganic sulfur species, the corresponding bitumen only contained organic sulfur. The organic sulfur content in the kerogens was lower than that in bitumen. After density separation, the kerogen was found to still contain a significant amount of inorganic impurities, such as pyrite, newly formed fluorides, titanium, zirconium and barium rich minerals, approximately 5 wt% in total. This may be caused by incomplete acid digestion, organic matter protection and neoformation. Pyrite, which is closely associated with organics, can also be observed through microscopy. The intimate association between pyrite and kerogen was possibly due to the bacterial oxidation of hydrocarbons, leading to the reduction of sulfate to sulfide which, in turn, led to the formation of pyrite.

5.2 Future work

1. Expandable clays in different geological end members from both the North Mine and Aurora Mine should be further studied. The <0.2 μm oil sands fraction should be collected in order to see the additional peak more clearly (Osacky, 2013). The vapor ethylene glycol preparation method may not be sufficient to induce clay expansion (Mosser-Ruck et al., 2005). The liquid ethylene glycol

preparation should be applied and the XRD patterns need to be compared to check for expandable clay in the Aurora Mine. 2. Nitrogen is a very important component of kerogen. Nitrogen compounds in different types of kerogen can be examined by XPS and nuclear magnetic resonance (NMR) imaging to see the nitrogen bonds in different kerogens (Kelemen, et al., 2007).

3. A non-aqueous extraction process needs to be chosen to study bitumen and solvent recovery for different oil sands geological end members during non-aqueous extraction. This may reveal correlations between bitumen/solvent recovery and types and quantities of clays and other inorganic minerals, as well as the types and chemical bonds of the kerogens.

4. Clay and kerogen behavior during non-aqueous extraction can be directly and indirectly studied. For instance, the attraction forces between clay/kerogen and bitumen/solvent can be carefully examined by atomic force microscopy (AFM). The capabilities of bitumen retention and solvent preservation in clays and kerogens can be studied by mixing clays and kerogens with bitumen and then extracting the bitumen, which can give general implications of their behavior during non-aqueous extraction.

References

Adams, J.J., Rostron, B.J., and Mendoza, C.A., 2004.Coupled fluid flow, heat and mass transport, and erosion in the Alberta basin: implications for the origin of the Athabasca oil sands. Canadian Journal of Earth Science, 41, 1077-1095.

AGS 105 soils. Soil colloids and the surface chemistry of soils. http://faculty.yc.edu/ycfaculty/ags105/week08/soil_colloids/soil_colloids_print.html (accessed August, 2013). Barillas, J.L.M., Dutra Jr., T.V., and Mata, W., 2006. Reservoir and operational parameters influence in SAGD process. Journal of Petroleum Science and Engineering, 54, 35.

Bayliss, P., and Levinson, A.A., 1976. Mineralogical review of the Athabasca oil sands deposits (lower cretaceous, Mannwille group). Bulletin of Canadian Petroleum Geology, 24, 211-214.

Benson, A. M., 1969. Filtration of solvent-water extracted tar sand. US Patent No. 3,459,653.

Bergaya, F., Theng, B.K.G., and Lagaly, G., (Ed.), 2006. Handbook of clay science. Elsevier Ltd.

Bernard, B.B., Bernard, H., and Brooks, J.M., 2009. Determination of total carbon, total organic carbon and inorganic carbon in sediments. TDI-Brooks International/B&B Laboratories Inc., Texas.

Berner, B.A., 1970. Sedimentary pyrite formation. American Journal of Science, 268, 1-23.

Bulmer, J.T., and Starr, J., (Ed.), 1979. Syncrude analytical methods for oil sands and bitumen processing. The Alberta Oil Sands Technology and Research Authority, 46-51.

Canadian Association of Petroleum Production (CAPP), 2012. The facts on oil sands, upstream dialogue.

Canfield, D.E., Lyons, T.W., and Raiswell, R., 1996. Amodel for iron deposition to euxinic Black Sea sediments. American Journal of Science, 296, 881-834.

Carrie, J., Sanei, H., and Stern, G., 2012. Standardisation of Rock–Eval pyrolysis for the analysis of recent sediments and soils. Organic Geochemistry, 46, 38-53.

Chang, Y., and Huang, W., 2008. Simulation of the fluorescence evolution of "live" oils from kerogens in a diamond anvil cell: Application to inclusion oils in terms of maturity and source. Geochimica et Cosmochimica Acta, 72 , 3771-3787.

Chong, J., Ng, S., Chung, K.H., Sparks, B.D., and Kotlyar, L.S., 2003. Impact of fines content on a warm slurry extraction process using model oilsands. Fuel, 82, 425.

Chung, F.H., 1974. Quantitative interpretation of X-ray diffraction patterns of mixtures. I. Matrix flushing method for quantitative multicomponent analysis. Journal of Applied Crystallography, 7, 519-525.

Correis, M., 1967. Relations possible entre l'état de conservation des élément figures de la matière organique et l'existence de gisements d'hydrocarbons. Rev. Inst. Fr. Petr. 22, 1285-1306.

Durand B., (Ed.), 1980. Kerogen: insoluble organic matter from sedimentary rocks, Editions Technip, France,

Eberl, D.D., 2003. User's guide to RockJock - a program for determining quantitative mineralogy from powder X-ray diffraction data. U.S. Geological Survey, Open-File Report No. 03-78.

Eslahpazir, R., Kupsta, M., Liu, Q., and Ivey, D.G., 2011. Sample preparation method for characterization of fine solids in Athabasca oil sands by electron microscopy. Energy Fuels, 25 (11), 5158-5164.

Gantz, D.E., and Hellwege, J.W., 1977. Solvent extraction of oil from tar sands utilizing a trichloroethylene solvent. US Patent No. 4,046,669.

Garven, G., 1989. A hydrogeologic model for the formation of the giant oil sands deposits of the western Canada sedimentary basin. American Journal of Science, 289, 105-166.

Geramian, M., Osacky, M., Zheng, L., Ivey, D.G., Liu, Q., and Etsell, T.H., 2012. Effect of various clay minerals on non-aqueous bitumen extraction. Presented at Oil Sands Conference, 28-30 August, Edmonton, Canada.

Guggenheim, S., and Martin, R.T., 1995. Definition of clay and clay mineral: joint report of the AIPEA nomenclature and CMS nomenclature committees. Clays and Clay Minerals, 43, 255-256 and Clay Minerals 30, 257-259.

Hooshiar, A., Uhlik, P., Liu, Q., Etsell, T.H., and Ivey, D.G., 2012. Clay minerals in nonaqueous extraction of bitumen from Alberta oil sands, Part 1: Nonaqueous extraction procedure. Fuel Processing Technology, 94, 80-85.

Hooshiar, A., Uhlik, P., Ivey, D.G., Liu, Q., and Etsell, T.H., 2012. Clay minerals in nonaqueous extraction of bitumen from Alberta oil sands, Part 2: Characterization of clay minerals. Fuel Processing Technology, 96, 183-94.

Hunt, J.M., 1967. The origin of petroleum in carbonate rocks. Carbonate Rocks-Physical and Chemical Aspects, 9(B), 225-251.

Hunt, J.M., 1996. Petroleum Geochemistry and Geology, 2nd Edition. W.H. Freeman Limited, New York.

Kaminsky, H.A.W., Etsell, T.H., Ivey, D.G., and Omotoso, O., 2008. Characterization of heavy minerals in Athabasca oil sands. Minerals Engineering, 21, 264-271.

Kaminsky, H.A.W., Etsell, T.H., Ivey, D.G., and Omotoso, O., 2009. Distribution of clay minerals in the process streams produced by the extraction of bitumen from Athabasca oil sands. The Canadian Journal of Chemical Engineering, 87 , 85-93.

Kelemen, S.R., Afeworki, M., Gorbaty, M.L., Sansone, M., Kwiatek, P.J., Walters, C.C., Freund, H., and Siskin M., 2007. Direct characterization of kerogen by X-ray and solid state ^{13}C nuclear magnetic resonance methods. Energy Fuels, 21 , 1548-1561.

Khursheed, A., 2011. Scanning Electron Microscope Optics and Spectrometers; World Scientific.

Kinghorn, R.R.F., and Rahman, M., 1980. The density separation of different maceral groups of organic matter dispersed in sedimentary rocks. Journal of Petroleum Geology, 2, 449-454.

Lafargue, E., Marquis, F., and Pillot, D., 1998. Rock-Eval 6 applications in hydrocarbon exploration, production, and soil contamination studies. Oil & Gas Science and Technology - Rev. IFP, 53 , 421-437.

Largeau, C., Derenne, S., Casadevall, E., Berkaloff, C., Corolleur, M., Lugardon, B., Raynaud, J.F., and Connan, J., 1990. Occurrence and origin of ultralaminar structures in amorphous kerogens of various source rocks and oil shales. Organic Geochemistry, 16 , 889-895.

Leung, H., and Phillips, C.R., 1985. Solvent-extraction of mined Athabasca oil sands. Industry and Engineering Chemistry Fundamentals, 24, 373.

Masliyah, J., Czarnecki, J., and Xu, Z., 2011. Handbook on theory and practice of bitumen recovery from Athabasca oil sands, Volume 1: Theoretical basis. Kingsley Knowledge Publication.

Moore, D.M., and Reynold, R.C. Jr., 1997. X-ray diffraction and the identification and analysis of clay minerals, Second edition. Oxford University Press, Oxford.

Mosser-Ruck, R., Devineau, K., Charpentier, D., and Cathelineau, M., 2005. Effects of ethylene glycol saturation protocols on XRD patterns: a critical review and discussion. Clay and Clay Minerals. 53 , 631-638.

Mossop, G.D., 1980. Geology of the Athabasca oil sands. Science, 207(4427), 145-152.

Nelson, D.W., and Sommers, L.E., 1996. Total carbon, organic carbon, and organic matter. In Sparks, D.L., (Ed.), Methods of soil analysis, Part 3-Chemical methods; Soil Science Society of America and American Society of Agronomy: Madison, Wisconsin, 961-1005.

Nikakhtari, H., Vagi, L., Choi, P., Liu, Q., and Gray, M.R., 2012. Solvent screening for non-aqueous extraction of Alberta oil sands. Canadian Journal of Chemical Engineering, 91, 6, 1153-1160.

Oberlin, A., Boulmier, J.L. and Villey, M., 1980. Electron microscopic study of kerogen microtexture. In Durand, B., (Ed.), Kerogen: insoluble organic matter from sedimentary rocks; Editions Technip, Paris, 191-241.

Oliver, F.H., 1955. A modified Unterzaucher method for the direct determination of combined oxygen. The Analyst, 80 (953), 593-594.

Omotoso, O., and Eberl, D., 2009. Sample preparation and data collection strategies for X-ray diffraction quantitative phase analysis of clay-bearing rocks. Proceedings of the 46th Annual Meeting of the Clay Minerals Society, 5-11 June, Billings, Montana.

Omotoso, O.E., and Mikula, R.J., 2004. High surface areas caused by smectitic interstratification of kaolinite and illite in Athabasca oil sands. Applied Clay Science, 25 , 37-47.

Osacky, M., Geramian M., Dyar, M., Sklute, E., Valter, M., Ivey, D.G., Liu, Q., and Etsell, T.H., 2013. Characterization of petrologic end members of oil sands from the Athabasca region, Alberta, Canada. Canadian Journal of Chemical Engineering, 91 (8), 1402-1415.

Osacky, M., Geramian, M., Ivey, D.G., Liu, Q., and Etsell, T.H., 2013. Mineralogical and chemical composition of petrologic end members of Alberta oil sands. Fuel, 113, 148-157.

Pembina Institute report, 2013. Understanding the impacts of oil sands production. http://pubs.pembina.org/reports/oilsands-key-facts-backgrounder-201301.pdf (accessed August, 2013).

Peters, K.E., and Cassa, M.R., 1994. Applied source rock geochemistry. In Magoon, L.B., and Dow, W.G. (Ed.), The petroleum system-from source to trap: American Association of Petroleum Geologists, Memoir, 60, 93-120.

Peters, K.E., and Moldowan, J.M., 1993. The biomarker guide: interpreting molecular fossils in petroleum and ancient sediments, Prentice Hall, Englewood Cliffs, New Jersey.

Ranger, M.J., and Gingras, M.K., 2007. Stratigraphy and sequence stratigraphic surfaces of the McMurray Formation. American Association of Petroleum Geologists, Hedburg Conference, 30 September - 3 October, Banff, Alberta.

Ranger, M.J., and Pemberton, S.G., 1997. Elements of a stratigraphic framework for the McMurray Formation in south Athabasca. In: Pemberton, S.G. and James, D.P., (Eds.), Petroleum geology of the cretaceous Mannville group, western Canada. Canadian Society of Petroleum Geologists, Memoir, Calgary, 18, 263-291.

Raiswell, R., and Canfield, D.E., 1998. Sources of iron for pyrite formation in marine sediments. American Journal of Science, 298, 219-245.

Sanei, H., Stasiuk, L.D., and Goodarzi, F., 2005. Petrological changes occurring in organic matter from recent lacustrine sediments during thermal alteration by Rock-Eval pyrolysis. Organic Geochemistry, 36 , 1190-1203.

Sawada, K., Kaiho, K., and Okano, K., 2012. Kerogen morphology and geochemistry at the Permian–Triassic transition in the Meishan section, South China: Implication for paleoenvironmental variation. Journal of Asian Earth Sciences 54-55, 78-90.

Schoonen, M.A.A., 2004. Mechanisms of sedimentary pyrite formation. Geological Society of America Special Papers, 379,117-134.

Senftle, J.T., 1986. Method and apparatus for characterizing kerogens. US patent 4616133A. Union Company of California, Los Angeles, CA.

Sisk, C., Diza, E., and Walls, J., 2010. 3D visualization and classification of pore structure and pore filling in gas shale. SPE Annual Technical Conference and Exhibition Florence, 19-22 September, Italy, 1-4.

Skjemstad, J.O., and Baldock, J.A., 2006. Total and organic carbon. In Carter M. R., and Gregorich, E. G. (Eds.), Soil sampling and methods of analysis; CRC Press, Boca Raton, 225-236.

Smith, D.K., Johnson, G.G. Jr., Scheible, W., Wims, A.M., Johnson, J.L. and Ullmann, G., 1987. Quantitative X-ray powder diffraction method using the full diffraction pattern: powder diffraction, 2, 73-77.

Sparks, B.D., and Meadus, F.W., 1988. Solvent extraction spherical agglomeration of oil sands. US Patent No. 4719008.

Środoń, J., Drits, V.A., McCarty, D.K., Hsieh, J.C.C., and Eberl, D.D., 2001. Quantitative X-ray diffraction analysis of clay-bearing rocks from random preparations. Clays Clay Minerals, 49, 514-528.

Środoń, J., 2002. Quantitative mineralogy of sedimentary rocks with emphasis on clays and with application to K-Ar dating. Mineralogical Magazine 66, 677-687.

Su, Y., Wang, J.Y., and Gates, I.D., 2013. SAGD well orientation in point bar oil sand deposit affects performance. Engineering Geology, 157, 79–92.

Tissot, B.P., and Welte, D.H., 1984. Petroleum formation and occurence. Springer-Verlag: Berlin, 160-198.

van Krevelen, D.W., 1961. Coal; Elsevier.

Wik, S., Sparks, B.D., Ng, S., Tu, Y., Li, Z., Chung, K.H., and Kotlyar, L.S., 2008. Effect of process water chemistry and particulate mineralogy on model oilsands separation using a warm slurry extraction process simulation. Fuel, 87, 1394-1412.

Yadav, T., and Vig, K.C., 1995. Retention behavior of bitumen in coals and shales of Indian sedimentary basins. Proceedings of Petrotech-95, 9-12 January, New Delhi, 235-244.

Zaccone, C., Sanei, H., Outridge, P.M. and Miano, T.M., 2011. Studying the humification degree and evolution of peat down a Holocene bog profile (Inuvik, NW Canada): a petrological and chemical perspective. Organic Geochemistry，42, 399–408.